MLL *fusion proteins and oncogenic* NRAS *cooperate to induce acute leukemia, at least partly through aberrant expression of* Hoxa9

The findings on the transformation of HF6 cells *in vitro* led to the hypothesis that *MLL* fusion proteins might cooperate with activation of Ras to induce *AML in vivo*. To test this hypothesis, the oncogenic potential of $NRAS^{G12V}$ (G12V) or STAT5A#2 (#2) to cooperate with *MLL-SEPT6* (MS6) or *MLL-ENL* short form was examined in the leukemogenesis assays *in vivo* (Supplementary Figure 1). STAT5A1*6 was not used owing to its too strong oncogenic potential *in vivo* as reported earlier.[36] The transduction efficiencies of $NRAS^{G12V}$, STAT5A#2 and *MLL-ENL* were 30–50, 20–40 and 5–10%, respectively, as determined by GFP expression (data not shown).

The mice receiving the BM cells transduced with *MLL-SEPT6* and $NRAS^{G12V}$ (MS6/G12V) died with significantly shorter latencies (26 ± 2.4 days; $P<0.05$, log-rank test) than the MS6/GFP mice that died of MPD (137 ± 9.0 days) as described earlier,[6] but, unexpectedly, the neo/G12V mice died as early as the MS6/G12V mice (31 ± 1.4 days) (Figure 4a, Table 1, and data not shown). The MS6/#2 mice died with significantly shorter latencies (82 ± 11 days; $P<0.05$, log-rank test) than the MS6/GFP mice, but as early as the neo/#2 mice (80 ± 8.0 days) (Figure 4a and Table 1). Notably, the phenotypes of the MS6/G12V mice were very different from those of the neo/G12V mice and from MPD in the MS6/GFP mice, whereas those of the MS6/#2 mice were rather similar to MPD in the MS6/GFP mice than those of the neo/#2 mice.

The morbid MS6/G12V mice showed hepatosplenomegaly with various ranges of leukocytosis, anemia and thrombocytopenia, whereas the morbid neo/G12V mice showed no hepatomegaly but mild splenomegaly, and severe pancytopenia (Figure 4b and Table 1). Histopathological analyses of the morbid MS6/G12V mice showed that immature myelomonocytic blasts accounted for more than 30% of BM cells, and severely infiltrated the spleen and the liver (Figures 4c and d, and data not shown). Immunophenotyping analyses of the BM cells also revealed that a majority of these cells expressed GFP, which indicated expression of $NRAS^{G12V}$, with high level of CD11b, intermediate level of Gr-1 (a myeloid differentiation marker also known as Ly-6G) and low level of c-Kit (CD117, the receptor of stem cell factor) (Figure 4e). In addition, Southern blot analysis of genomic DNAs derived from the spleens of the MS6/G12V mice showed oligoclonal bands of proviral integration (Figure 4g). These results indicated that the MS6/G12V mice developed *AML* similar to the mice receiving BM cells transduced with *MLL-SEPT6* and *FLT3*-ITD, as described earlier.[6] In contrast, the morbid neo/G12V mice showed extremely hypocellular marrows and extramedullary hematopoiesis in the spleen, where a majority of the cells did not express Ly5.1 (Figure 4f), with little expression of *Hoxa9* in comparison with the morbid MS6/G12V mice (Supplementary Figure 3a). Thus, this finding suggested that, in our leukemogenesis assays under lethal conditioning, *NRAS* might develop BM aplasia presumably due to engraftment failure. Meanwhile, the MS6/#2 mice died of MPD, showing myeloid hyperplasia consisting predominantly of mature granulocytic elements in the BM cells, where a very small population (1.0%) expressed STAT5A#2, with splenomegaly similar to the MS6/GFP mice (Figures 4b–d, and Table 1). The neo/#2 mice showed neither hepatosplenomegaly nor hematological abnormalities in the peripheral blood, but relative myeloid hyperplasia in the BM, where only a small population (9.4%) expressed STAT5A#2 (Figures 4b and f, data not shown and Table 1), thus implying that STAT5A#2 might induce lethal BM abnormality owing to paracrine expression of some cytokines as in the earlier report using STAT5A1*6.[36]

To generalize leukemogenic cooperation between *MLL* fusion proteins and oncogenic *NRAS* and avoid the early death caused by transduction of $NRAS^{G12V}$, the BM cells transduced with *MLL-ENL* and/or oncogenic *NRAS* were also transplanted into recipient mice under sublethal conditioning. The *MLL-ENL* short form was used for leukemogenesis assays under sublethal conditioning with oncogenic *NRAS* ($NRAS^{G12V}$), in which retroviral vectors were exchanged, so that the expression of GFP indicated that of *MLL-ENL* (Supplementary Figure 1). These leukemogenesis assays under sublethal conditioning confirmed that the combination of *MLL-ENL* and $NRAS^{G12V}$ reproduced *AML*, and that *MLL-ENL* (and puro) induced the phenotype of MPD (Figures 5a, b and d, and Table 1). Meanwhile, $NRAS^{G12V}$

Table 1 Characteristics of the morbid mice transplanted with hematopoietic progenitors transduced with *MLL* fusion genes or *Hoxa9*, and/or either $NRAS^{G12V}$ or STAT5A #2

Mouse	*Latency (days)*	*Liver (g)*	*Spleen (g)*	*Thymus (g)*	*WBC (per μl)*	*Hb (g per 100 ml)*	*Plt (× 10^4 per μl)*
Lethal conditioning							
MS6/G12V ($n=6$)	26 ± 2.4	1.60 ± 0.35	0.31 ± 0.07	0.020 ± 0.012	74 600 ± 62 900	4.2 ± 1.0	4.0 ± 3.9
MS6/#2 ($n=3$)[a]	82 ± 11	0.98 ± 0.43	0.32 ± 0.03	0.019 ± 0.006	73 100	5.3	4.4
MS6/GFP ($n=6$)	137 ± 9.0	1.54 ± 0.69	0.26 ± 0.09	0.037 ± 0.005	309 000 ± 263 000	7.0 ± 6.6	8.0 ± 5.7
neo/G12V ($n=6$)	31 ± 1.4	1.04 ± 0.25	0.25 ± 0.08	0.030 ± 0.030	4600 ± 1800	2.5 ± 0.3	0.5 ± 0.4
neo/#2 ($n=3$)[a]	80 ± 8.0	0.66 ± 0.16	0.08 ± 0.06	0.011 ± 0.001	9800	18.8	58.2
neo/GFP ($n=3$)	NA	1.36 ± 0.11	0.09 ± 0.01	0.051 ± 0.010	12 000 ± 4700	14.7 ± 0.6	81 ± 13
A9/G12V ($n=4$)	28 ± 7.5	1.93 ± 0.56	0.44 ± 0.16	0.033 ± 0.030	76 300 ± 56 700	4.5 ± 2.7	1.0 ± 0.6
A9/GFP ($n=6$)	NA	NT	NT	NT	21 200 ± 5400	17.3 ± 2.4	66 ± 4.7
puro/GFP ($n=3$)	NA	1.48 ± 0.21	0.06 ± 0.01	0.049 ± 0.022	12 000 ± 3400	13.6 ± 1.5	81 ± 19
Sublethal conditioning							
MEs/G12V ($n=10$)	21 ± 3.9	2.56 ± 0.45	0.51 ± 0.10	0.043 ± 0.020	164 000 ± 131 000	7.2 ± 2.5	11 ± 4.5
MEs/puro ($n=5$)	89 ± 11	1.89 ± 0.58	0.44 ± 0.11	0.043 ± 0.006	99 000 ± 53 000	7.4 ± 2.9	9.1 ± 3.1
GFP/G12V ($n=5$)[b]	89 ± 10	0.90 ± 0.31	0.06 ± 0.03	0.63 ± 0.35	22 000 ± 1000	13.6 ± 1.7	97
GFP/puro ($n=3$)	NA	NT	NT	NT	NT	NT	NT

Abbreviations: GFP, green fluorescent protein; Hb, hemoglobin; MEs, *MLL-ENL* short form; NA, not applicable; NT, not tested; Plt, platelet; WBC, white blood cell.
Averages with s.d. are shown.
[a]Blood cell counts of only one morbid mouse were performed.
[b]One mouse developing acute leukemia and thymoma was excluded, owing to the remarkably increased number of WBCs and hepatosplenomegaly. The platelet count of only one morbid mouse was determined.

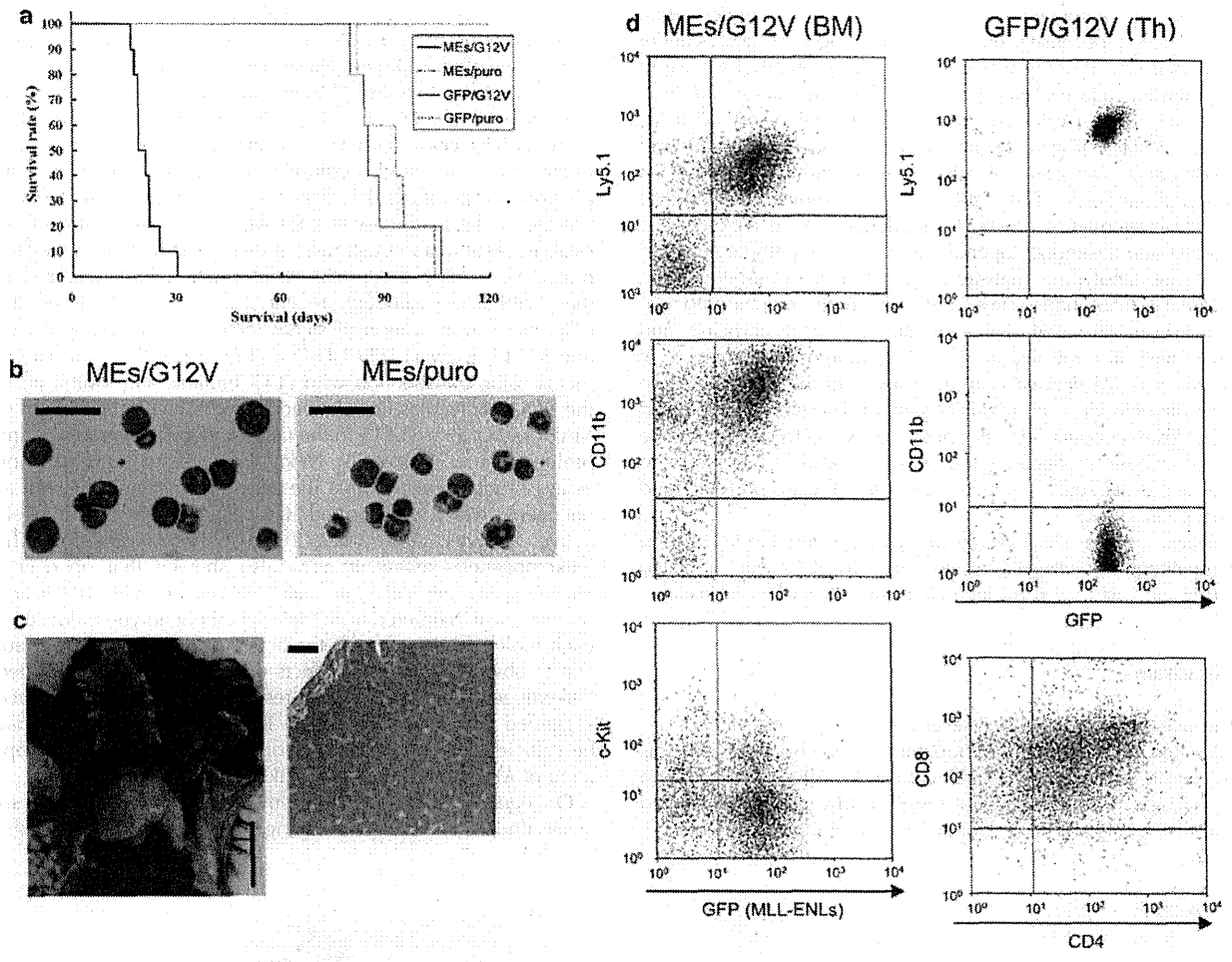

Figure 5 Leukemogenesis assays under sublethal conditioning using *mixed-lineage-leukemia/eleven nineteen leukemia* (*MLL-ENL*) and $NRAS^{G12V}$. (**a**) Survival curves of mice transplanted with a short form of *MLL-ENL* (MEs) and $NRAS^{G12V}$ (MEs/G12V) ($n=10$), MEs/puro ($n=5$), GFP/G12V ($n=5$) and green fluorescent protein (GFP)/puro ($n=3$). (**b**) Representative cytospin preparations of bone marrow (BM) cells obtained from morbid MEs/G12V and MEs/puro mice. The cells were stained with Wright-Giemsa. Original magnification 200×; Scale bars 30 μm. (**c**) Representative histopathologic images of thymus obtained from the GFP/G12V mouse. A paraffin section of the thymus was stained with hematoxylin and eosin (H&E). Original magnification, ×40; vertical and horizontal scale bars, 1 cm and 200 μm, respectively. (**d**) Immunophenotype of BM and thymic (Th) cells obtained from representative morbid MEs/G12V and GFP/G12V mice. The dot plots show each surface antigen labeled with a corresponding monoclonal antibody versus expression of GFP or CD4. Ly5.1, CD11b, CD4, and c-Kit and CD8 were labeled with phycoerythrin (PE)-conjugated and allophycocyanin (APC)-conjugated monoclonal antibodies, respectively.

(and GFP) led to thymoma, sometimes together with leukocytosis, with a long latency (Figures 5a, c and d, and Table 1). In addition, to examine the possibility that the phenotypes associated with STAT5A#2 might change, similar to oncogenic *NRAS*, the BM cells transduced with STAT5A#2 (in pMYs-IRES-EGFP) and/or *MLL-SEPT6* (in pMXs-neo) were again transplanted into recipient mice under sublethal conditioning. Within an observation period of 160 days, two of three neo/#2 mice under sublethal conditioning died with longer latencies (134 and 139 days) and showed the same phenotype of myeloid hyperplasia in the BM, where a small population (15%) expressed STAT5A#2, although these had different phenotypes of pancytopenia and splenomegaly (Supplementary Figure 3b and data not shown). In contrast, two of three MS6/#2 mice and all of the three MS6/GFP mice survived and showed no hematological abnormalities in the peripheral blood, whereas one of the MS6/#2 mice died (125 day) but could not be analyzed because of post-mortem change, within the observation period. Histopathological analysis of one MS6/#2 mouse, which was killed 150 days after the transplantation, showed no significant hepatosplenomegaly but mild myeloid hyperplasia in the BM (data not shown). Only 30% of the BM cells were positive for donor-derived Ly-5.1, and 7% of the BM cells were positive for GFP, indicating expression of STAT5A#2 (Supplementary Figure 3c), whereas reverse transcriptase-PCR analysis of the BM cells gave very weak signals of *MLL-SEPT6* after 30 cycles (data not shown), but clearly visible signals after 35 cycles (Supplementary Figure 3c). Therefore, sublethal conditioning seemed to be inappropriate for leukemogenesis assays using oncogenes, such as *MLL-SEPT6* and STAT5A#2, which had relatively weak oncogenic potential in comparison with *MLL-ENL* and $NRAS^{G12V}$.

Finally, we examined whether *Hoxa9* may be involved in cooperation between the *MLL* fusion protein and oncogenic *NRAS in vivo*, such as in transformation assays *in vitro*. The leukemogenesis assays using the BM cells transduced with

Hoxa9 and oncogenic *NRAS* were carried out under lethal conditioning, because preliminary leukemogenesis assays under sublethal conditioning were unsuccessful probably because of engraftment failure (data not shown). The combination of *Hoxa9* and $NRAS^{G12V}$ (A9/G12V) led to death with short latencies (28 ± 7.5 days) (Figure 6a and Table 1), whereas *Hoxa9* (and GFP) *per se* induced no lethal disease within 120 days, as reported earlier.[37] The A9/G12V mice showed remarkable hepatosplenomegaly and had a tendency toward leukocytosis, anemia and thrombocytopenia (Table 1). Histopathological and immunophenotyping analyses of the BM cells revealed that the A9/G12V mice had a few, but prominent, myelomonocytic blasts (Figure 6b), with high expression of CD11b and Gr-1, and low level of c-Kit (Figure 6c). A Southern blot analysis of genomic DNAs derived from the spleens of the A9/G12V mice gave oligoclonal bands (data not shown). These results indicated that *Hoxa9* cooperated with oncogenic *NRAS* to rapidly induce lethal myeloid malignancy that was not identical but similar to the acute leukemia induced by *MLL* fusion proteins and oncogenic *NRAS*.

Taken together, these results *in vivo* suggested that *MLL* fusion proteins rapidly induce acute leukemia together with activated *NRAS*, at least in part through aberrant expression of *Hoxa9*.

Discussion

The present study provides several evidences that *MLL*-fusion-mediated leukemogenesis cooperated synergistically with Ras activation, but not with STAT5 activation. Although all known *MLL* fusion proteins were not tested in this study, we showed that this synergistic cooperation was not limited to the specific *MLL* fusion, using two different well-characterized types of *MLL* fusion proteins. In the light of the role of FLT3 mutations in *MLL*-fusion-mediated leukemogenesis described earlier,[6] signaling pathways downstream of FLT3 mutations were analyzed in the transfectants of HF6, a cell line expressing *MLL-SEPT6*. The immortalized cells, such as HF6 and A9G, used in this study might have acquired additional mutations. However, the phenotypes including IL-3 dependency, expression patterns of lineage markers and growth rates were not changed since their establishment (data not shown), thus suggesting that at least no mutations leading to critical transformation had occurred in these cell lines. Although recent studies have disclosed the differences in activation of signal molecules, including MAPK and STAT5, between *FLT3*-TKD and *FLT3*-ITD,[24,38] our experiments using transduction with FLT3 mutants and inhibition of the signal molecules first showed a crucial role of activation of MAPK rather than STAT5 in the factor-independent survival and proliferation of HF6 cells. Next, the myeloid transformation assays *in vitro* revealed that the activation of Raf-1, as well as oncogenic *NRAS*, transformed HF6 cells, but that constitutively active mutants (1*6 and #2) of STAT5A did not. The leukemogenesis assays *in vivo* also showed that oncogenic *NRAS* rapidly induced acute leukemia together with *MLL* fusion proteins, which differed from the original phenotype induced by each molecule. In contrast, the active STAT5A mutant did not confer obvious synergistic effects on the *MLL*-fusion-mediated leukemogenesis. Thus, these results *in vitro* and *in vivo* suggested that activation of the Ras/Raf/MAPK pathway may be sufficient for the transformation of HF6 cells and development of *MLL*-fusion-mediated leukemia.

Oncogenic *NRAS* induced thymoma in the leukemogenesis assays under sublethal conditioning, which is consistent with the

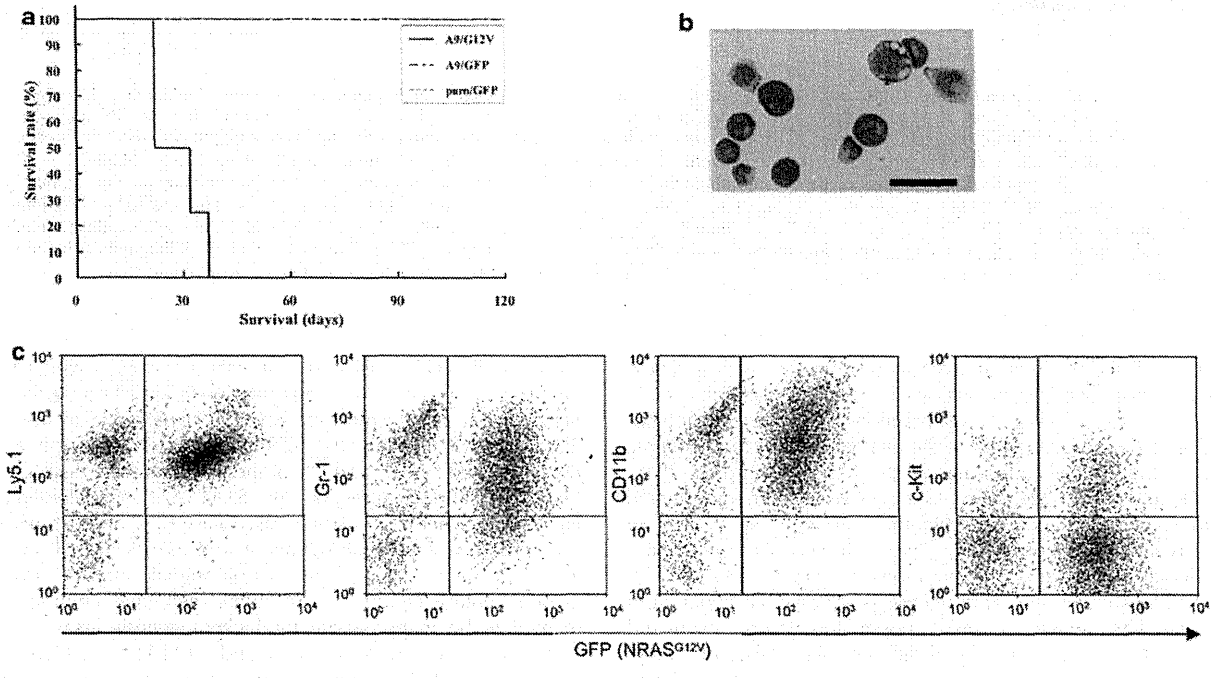

Figure 6 Leukemogenesis induced by *Hoxa9* and oncogenic neuroblastoma RAS viral (v-ras) oncogene homolog (*NRAS*) under lethal conditioning. (**a**) Survival curves of mice transplanted with *Hoxa9* and $NRAS^{G12V}$ (A9/G12V; $n=4$), A9/green fluorescent protein (GFP) ($n=6$) and puro/GFP ($n=3$). (**b**) Representative cytospin preparations of bone marrow (BM) cells obtained from morbid A9/G12V mice. The cells were stained with Wright-Giemsa. Original magnification, × 200; scale bar, 30 μm. (**c**) Immunophenotype of BM cells obtained from representative morbid A9/G12V mice. The dot plots show each surface antigen labeled with a corresponding monoclonal antibody versus expression of GFP. Ly5.1, Gr-1, CD11b, and c-Kit were labeled with phycoerythrin (PE)-conjugated and allophycocyanin (APC)-conjugated monoclonal antibodies, respectively.

development of T-lymphoma by *FLT3*-TKD in our experimental system (Ono *et al.*, unpublished data), whereas it led to the development of BM aplasia in our leukemogenesis assays under lethal conditioning. This difference in the disease phenotypes implies that forced expression of oncogenic *NRAS* in BM progenitors might be involved in its inhibitory effects on the engraftment of radioprotective cells as well as the antiproliferative effect of oncogenic *NRAS* in the early phase of the transplantation.[39] These disease phenotypes were also different from the development of MPD in the earlier reports.[39,40] This discrepancy might be due to the differences in the experimental systems, such as the retroviral transduction and mice strains. Meanwhile, the BM progenitors transduced with *Hoxa9* and *NRAS*^{G12V} seemed to result in engraftment failure under sublethal conditioning, but these rapidly developed myeloid malignancy under lethal conditioning. A recent study using BM transplantation showed the possibility of drastic fluctuation in the engraftment of donor cells receiving pathological modification under sublethal conditioning;[41] hence, our unsuccessful results under sublethal conditioning might be associated with some instability of the transplantation.

Our leukemogenesis assays showed a definitively synergistic cooperation between *MLL* fusion proteins and oncogenic *NRAS* in the acceleration of disease onset and change of the phenotypes. Interestingly, the synergistic cooperation between *MLL* fusion proteins and Ras/Raf/MAPK activation closely correlated with recent clinical studies reporting the frequent coincidence of *MLL* fusion genes and mutations of *RAS*[20] or *RAF*.[42] It was reported that the additional expression of oncogenic *KRAS* induced an acute promyelocytic leukemia-like disease in transgenic mice expressing promyelocytic leukemia/retinoic acid receptor-α with an increased penetrance and decreased latency, although neither the penetrance nor the latency was significantly different from those in mice that died of MPD by expression of oncogenic *KRAS* alone.[43] Other groups recently reported that the combination of oncogenic *NRAS* and *MLL-AF9*[44] or *MLL-ENL*[45] is capable of developing *AML*, and that induced repression of oncogenic *NRAS* on the combination reverted *AML* to MPD by the *MLL* fusion gene (*MLL-AF9*) alone.[44] Although our findings that *MLL* fusion proteins and oncogenic *NRAS* cooperate to induce *AML* confirmed these notions, the present study further analyzed the involvement of *Hoxa9* and Raf, downstream of the cooperation between *MLL* fusion proteins and oncogenic *NRAS*. The myeloid transformation assays *in vitro* showed that the activation of Raf-1, as well as oncogenic *NRAS*, transformed A9G, a cell line expressing *Hoxa9*. The leukemogenesis assays *in vivo* also showed that *Hoxa9* and oncogenic *NRAS* rapidly developed myeloid malignancy. These results *in vitro* and *in vivo* suggested that, as downstream molecules, *Hoxa9* and Raf may have important roles in the synergistic leukemogenesis by *MLL* fusion proteins and oncogenic *NRAS*.

Our findings suggest a possible model of *MLL*-fusion-mediated leukemogenesis that was essentially recapitulated by *Hoxa9* expression and Ras/Raf/MAPK activation (Figure 7). In the context of secondary genetic alterations, such as *FLT3* mutations, this model explains the clinical features of acute leukemia with 11q23 translocations. First, overexpression, as well as TKD mutations, of *FLT3* frequently detected in the *MLL*-rearranged infant acute leukemia may be involved in the leukemogenesis mainly through activation of Ras/Raf/MAPK, because several studies reported that the signaling pathway of wild-type *FLT3* is similar to *FLT3*-TKD rather than *FLT3*-ITD.[24,38] Second, besides *FLT3*, other unknown molecular pathways that lead to the activation of Ras/Raf/MAPK might also be involved in

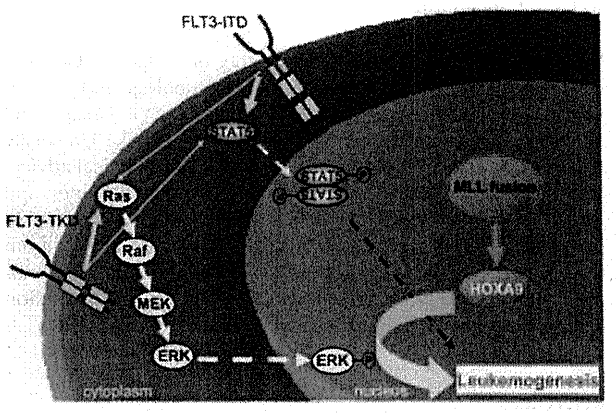

Figure 7 A model of *mixed-lineage-leukemia* (*MLL*)-mediated leukemogenesis together with secondary genetic alterations. *MLL* fusion protein and secondary genetic alterations cooperate to induce acute leukemia through synergistic molecular crosstalk between aberrant expression of *Hox* genes, including *Hoxa9*, and the activation of Ras/Raf/mitogen-activated protein kinase (MAPK). Other signaling pathways, including signal transducer and activator of transcription 5 (STAT5) activation, only additively affect the leukemogenic potential.

the *MLL*-rearranged leukemia carrying no known genetic alterations, as *FLT3* alterations are not found very frequently in most *MLL*-rearranged leukemia except in infants.[46,47] Meanwhile, in the context of *MLL* fusion proteins, we analyzed the role of the *Hoxa9*-mediated pathway leading to leukemogenesis. Recent studies revealed that one of the *Hox*-cofactor molecules, *Meis1*, is an essential molecule involved in normal hematopoiesis[48] as well as *Hoxa9*-mediated leukemogenesis.[49] However, our experimental system[6] using BM cells transduced with *MLL* fusion proteins did not detect any significant upregulation of *Meis1* in comparison with the mock transduction as reported earlier,[50] in contrast with the findings by other groups.[14] Therefore, we focused on *Hoxa9*, one of the key molecules directly upregulated by *MLL* fusion proteins. Interestingly, a recent study showed that the combination of *Hoxa9* and *Meis1* cooperated with *Trib1*, which enhanced the phosphorylation of ERK, to induce acute leukemia in the BM transplantation assays.[51] Their study is not inconsistent with our findings; thus, the *HOX* and Ras/Raf/MAPK axes may have central roles in the molecular network of *MLL*-mediated leukemogenesis, which might be additively affected by other pathways, such as activation of STAT5 (Figure 7). In addition, at least, endogenous expression of *Meis1* in A9G cells is also considered to be important in this network, but further analysis will be required to clarify the role of *Meis1* in the collaboration between *HOX* and MAPK axes.

Conclusion

This study suggests that *MLL* fusion proteins synergistically cooperate with Ras/Raf/MAPK activation in leukemogenesis, at least partly through the upregulation of *Hoxa9*. Future studies analyzing the molecular crosstalk between *Hoxa9* and the Ras/Raf/MAPK cascade are expected to provide novel insights into the molecular mechanism of *MLL*-fusion-mediated leukemogenesis.

Conflict of interest

The authors declare no conflict of interest.

Acknowledgements

We thank Dr Guy Sauvageau (Laboratory of Molecular Genetics of Stem Cells, Institute for Research in Immunology and Cancer, Canada) for the plasmid harboring a fragment of *Hoxa9*, and Dr Yusuke Satoh (Hematology and Oncology, Osaka University Graduate School of Medicine, Osaka, Japan) for technical advice. We are also grateful to R&D Systems for providing cytokines, and Brian Quinn for language assistance. This work was supported in part by Chugai Pharmaceutical Company Ltd, Grants-in-Aid from the Ministry of Education, Culture, Sports, Science, and Technology in Japan, the Novartis Foundation (Japan) for the Promotion of Science and the Japan Leukaemia Research Fund.

References

1 Vogelstein B, Kinzler KW. Cancer genes and the pathways they control. *Nat Med* 2004; **10**: 789–799.
2 Look AT. Oncogenic transcription factors in the human acute leukemias. *Science* 1997; **278**: 1059–1064.
3 Rowley JD. The critical role of chromosome translocations in human leukemias. *Annu Rev Genet* 1998; **32**: 495–519.
4 Gilliland DG, Tallman MS. Focus on acute leukemias. *Cancer Cell* 2002; **1**: 417–420.
5 Kelly LM, Kutok JL, Williams IR, Boulton CL, Amaral SM, Curley DP *et al.* PML/RARalpha and FLT3-ITD induce an APL-like disease in a mouse model. *Proc Natl Acad Sci USA* 2002; **99**: 8283–8288.
6 Ono R, Nakajima H, Ozaki K, Kumagai H, Kawashima T, Taki T *et al.* Dimerization of MLL fusion proteins and FLT3 activation synergize to induce multiple-lineage leukemogenesis. *J Clin Invest* 2005; **115**: 919–929.
7 Schessl C, Rawat VP, Cusan M, Deshpande A, Kohl TM, Rosten PM *et al.* The *AML1-ETO* fusion gene and the FLT3 length mutation collaborate in inducing acute leukemia in mice. *J Clin Invest* 2005; **115**: 2159–2168.
8 Stubbs MC, Kim YM, Krivtsov AV, Wright RD, Feng Z, Agarwal J *et al.* MLL-AF9 and FLT3 cooperation in acute myelogenous leukemia: development of a model for rapid therapeutic assessment. *Leukemia* 2008; **22**: 66–77.
9 Watanabe-Okochi N, Kitaura J, Ono R, Harada H, Harada Y, Komeno Y *et al.* AML1 mutations induced MDS and MDS/AML in a mouse BMT model. *Blood* 2008; **111**: 4297–4308.
10 Ayton PM, Cleary ML. Molecular mechanisms of leukemogenesis mediated by MLL fusion proteins. *Oncogene* 2001; **20**: 5695–5707.
11 Meyer C, Kowarz E, Hofmann J, Renneville A, Zuna J, Trka J *et al.* New insights to the MLL recombinome of acute leukemias. *Leukemia* 2009; **23**: 1490–1499.
12 Yokoyama A, Somervaille TC, Smith KS, Rozenblatt-Rosen O, Meyerson M, Cleary ML. The menin tumor suppressor protein is an essential oncogenic cofactor for MLL-associated leukemogenesis. *Cell* 2005; **123**: 207–218.
13 Daser A, Rabbitts TH. Extending the repertoire of the *mixed-lineage leukemia* gene *MLL* in leukemogenesis. *Genes Dev* 2004; **18**: 965–974.
14 Hess JL. MLL: a histone methyltransferase disrupted in leukemia. *Trends Mol Med* 2004; **10**: 500–507.
15 Corral J, Lavenir I, Impey H, Warren AJ, Forster A, Larson TA *et al.* An *MLL-AF9* fusion gene made by homologous recombination causes acute leukemia in chimeric mice: a method to create fusion oncogenes. *Cell* 1996; **85**: 853–861.
16 Drynan LF, Pannell R, Forster A, Chan NM, Cano F, Daser A *et al.* MLL fusions generated by Cre-loxP-mediated *de novo* translocations can induce lineage reassignment in tumorigenesis. *EMBO J* 2005; **24**: 3136–3146.
17 Wang J, Iwasaki H, Krivtsov A, Febbo PG, Thorner AR, Ernst P *et al.* Conditional *MLL-CBP* targets GMP and models therapy-related myeloproliferative disease. *EMBO J* 2005; **24**: 368–381.
18 Chen W, Li Q, Hudson WA, Kumar A, Kirchhof N, Kersey JH. A murine *MLL-AF4* knock-in model results in lymphoid and myeloid deregulation and hematologic malignancy. *Blood* 2006; **108**: 669–677.
19 Taketani T, Taki T, Sugita K, Furuichi Y, Ishii E, Hanada R *et al.* FLT3 mutations in the activation loop of tyrosine kinase domain are frequently found in infant ALL with *MLL* rearrangements and pediatric ALL with hyperdiploidy. *Blood* 2004; **103**: 1085–1088.
20 Liang DC, Shih LY, Fu JF, Li HY, Wang HI, Hung IJ *et al.* K-Ras mutations and N-Ras mutations in childhood acute leukemias with or without mixed-lineage leukemia gene rearrangements. *Cancer* 2006; **106**: 950–956.
21 Gilliland DG, Griffin JD. The roles of FLT3 in hematopoiesis and leukemia. *Blood* 2002; **100**: 1532–1542.
22 Armstrong SA, Staunton JE, Silverman LB, Pieters R, den Boer ML, Minden MD *et al.* *MLL* translocations specify a distinct gene expression profile that distinguishes a unique leukemia. *Nat Genet* 2002; **30**: 41–47.
23 Murata K, Kumagai H, Kawashima T, Tamitsu K, Irie M, Nakajima H *et al.* Selective cytotoxic mechanism of GTP-14564, a novel tyrosine kinase inhibitor in leukemia cells expressing a constitutively active Fms-like tyrosine kinase 3 (FLT3). *J Biol Chem* 2003; **278**: 32892–32898.
24 Choudhary C, Schwable J, Brandts C, Tickenbrock L, Sargin B, Kindler T *et al.* AML-associated Flt3 kinase domain mutations show signal transduction differences compared with Flt3 ITD mutations. *Blood* 2005; **106**: 265–273.
25 Nosaka T, Kawashima T, Misawa K, Ikuta K, Mui AL, Kitamura T. STAT5 as a molecular regulator of proliferation, differentiation and apoptosis in hematopoietic cells. *EMBO J* 1999; **18**: 4754–4765.
26 Schubbert S, Shannon K, Bollag G. Hyperactive Ras in developmental disorders and cancer. *Nat Rev Cancer* 2007; **7**: 295–308.
27 Ariyoshi K, Nosaka T, Yamada K, Onishi M, Oka Y, Miyajima A *et al.* Constitutive activation of STAT5 by a point mutation in the SH2 domain. *J Biol Chem* 2000; **275**: 24407–24413.
28 Onishi M, Nosaka T, Misawa K, Mui AL, Gorman D, McMahon M *et al.* Identification and characterization of a constitutively active STAT5 mutant that promotes cell proliferation. *Mol Cell Biol* 1998; **18**: 3871–3879.
29 Kitamura T, Koshino Y, Shibata F, Oki T, Nakajima H, Nosaka T *et al.* Retrovirus-mediated gene transfer and expression cloning: powerful tools in functional genomics. *Exp Hematol* 2003; **31**: 1007–1014.
30 Kroon E, Krosl J, Thorsteinsdottir U, Baban S, Buchberg AM, Sauvageau G. Hoxa9 transforms primary bone marrow cells through specific collaboration with Meis1a but not Pbx1b. *EMBO J* 1998; **17**: 3714–3725.
31 Sakaue-Sawano A, Kurokawa H, Morimura T, Hanyu A, Hama H, Osawa H *et al.* Visualizing spatiotemporal dynamics of multicellular cell-cycle progression. *Cell* 2008; **132**: 487–498.
32 Calvo KR, Sykes DB, Pasillas M, Kamps MP. Hoxa9 immortalizes a granulocyte-macrophage colony-stimulating factor-dependent promyelocyte capable of biphenotypic differentiation to neutrophils or macrophages, independent of enforced meis expression. *Mol Cell Biol* 2000; **20**: 3274–3285.
33 Ono R, Ihara M, Nakajima H, Ozaki K, Kataoka-Fujiwara Y, Taki T *et al.* Disruption of *Sept6*, a fusion partner gene of *MLL*, does not affect ontogeny, leukemogenesis induced by *MLL-SEPT6*, or phenotype induced by the loss of *Sept4*. *Mol Cell Biol* 2005; **25**: 10965–10978.
34 Nosaka T, van Deursen JM, Tripp RA, Thierfelder WE, Witthuhn BA, McMickle AP *et al.* Defective lymphoid development in mice lacking Jak3. *Science* 1995; **270**: 800–802.
35 Moriggl R, Gouilleux-Gruart V, Jähne R, Berchtold S, Gartmann C, Liu X *et al.* Deletion of the carboxyl-terminal transactivation domain of MGF-STAT5 results in sustained DNA binding and a dominant negative phenotype. *Mol Cell Biol* 1996; **16**: 5691–5700.
36 Schwaller J, Parganas E, Wang D, Cain D, Aster JC, Williams IR *et al.* STAT5 is essential for the myelo- and lymphoproliferative disease induced by TEL/JAK2. *Mol Cell* 2000; **6**: 693–704.
37 Nakamura T, Largaespada DA, Shaughnessy Jr JD, Jenkins NA, Copeland NG. Cooperative activation of Hoxa and Pbx1-related genes in murine myeloid leukaemias. *Nat Genet* 1996; **12**: 149–153.
38 Grundler R, Miething C, Thiede C, Peschel C, Duyster J. FLT3-ITD and tyrosine kinase domain mutants induce 2 distinct phenotypes in a murine bone marrow transplantation model. *Blood* 2005; **105**: 4792–4799.

39 MacKenzie KL, Dolnikov A, Millington M, Shounan Y, Symonds G. Mutant N-ras induces myeloproliferative disorders and apoptosis in bone marrow repopulated mice. *Blood* 1999; **93**: 2043–2056.
40 Parikh C, Subrahmanyam R, Ren R. Oncogenic NRAS rapidly and efficiently induces CMML- and AML-like diseases in mice. *Blood* 2006; **108**: 2349–2357.
41 Santaguida M, Schepers K, King B, Sabnis AJ, Forsberg EC, Attema JL *et al.* JunB protects against myeloid malignancies by limiting hematopoietic stem cell proliferation and differentiation without affecting self-renewal. *Cancer Cell* 2009; **15**: 341–352.
42 Christiansen DH, Andersen MK, Desta F, Pedersen-Bjergaard J. Mutations of genes in the receptor tyrosine kinase (RTK)/RAS-BRAF signal transduction pathway in therapy-related myelodysplasia and acute myeloid leukemia. *Leukemia* 2005; **19**: 2232–2240.
43 Chan IT, Kutok JL, Williams IR, Cohen S, Moore S, Shigematsu H *et al.* Oncogenic K-ras cooperates with PML-RAR alpha to induce an acute promyelocytic leukemia-like disease. *Blood* 2006; **108**: 1708–1715.
44 Kim WI, Matise I, Diers MD, Largaespada DA. RAS oncogene suppression induces apoptosis followed by more differentiated and less myelosuppressive disease upon relapse of acute myeloid leukemia. *Blood* 2009; **113**: 1086–1096.
45 Zuber J, Radtke I, Pardee TS, Zhao Z, Rappaport AR, Luo W *et al.* Mouse models of human AML accurately predict chemotherapy response. *Genes Dev* 2009; **23**: 877–889.
46 Chillon MC, Fernandez C, Garcia-Sanz R, Balanzategui A, Ramos F, Fernandez-Calvo J *et al.* FLT3-activating mutations are associated with poor prognostic features in AML at diagnosis but they are not an independent prognostic factor. *Hematol J* 2004; **5**: 239–246.
47 Bacher U, Haferlach C, Kern W, Haferlach T, Schnittger S. Prognostic relevance of FLT3-TKD mutations in AML: the combination matters–an analysis of 3082 patients. *Blood* 2008; **111**: 2527–2537.
48 Hisa T, Spence SE, Rachel RA, Fujita M, Nakamura T, Ward JM *et al.* Hematopoietic, angiogenic and eye defects in Meis1 mutant animals. *EMBO J* 2004; **23**: 450–459.
49 Wong P, Iwasaki M, Somervaille TC, So CW, Cleary ML. Meis1 is an essential and rate-limiting regulator of MLL leukemia stem cell potential. *Genes Dev* 2007; **21**: 2762–2774.
50 Horton SJ, Grier DG, McGonigle GJ, Thompson A, Morrow M, De Silva I *et al.* Continuous MLL-ENL expression is necessary to establish a 'Hox Code' and maintain immortalization of hematopoietic progenitor cells. *Cancer Res* 2005; **65**: 9245–9252.
51 Jin G, Yamazaki Y, Takuwa M, Takahara T, Kaneko K, Kuwata T *et al.* Trib1 and Evi1 cooperate with Hoxa and Meis1 in myeloid leukemogenesis. *Blood* 2007; **109**: 3998–4005.

Supplementary Information accompanies the paper on the Leukemia website (http://www.nature.com/leu)

THE JOURNAL OF BIOLOGICAL CHEMISTRY VOL. 284, NO. 44, pp. 30673–30683, October 30, 2009

Expression Levels of Histone Deacetylases Determine the Cell Fate of Hematopoietic Progenitors*[S]

Received for publication, July 8, 2009, and in revised form, September 2, 2009 Published, JBC Papers in Press, September 7, 2009, DOI 10.1074/jbc.M109.042242

Taeko Wada[‡1], Jiro Kikuchi[‡], Noriko Nishimura[‡], Rumi Shimizu[‡], Toshio Kitamura[§], and Yusuke Furukawa[‡2]

From the [‡]Division of Stem Cell Regulation, Center for Molecular Medicine, Jichi Medical School, Tochigi 329-0498 and the [§]Division of Cellular Therapy and Division of Stem Cell Signaling, Institute of Medical Science, University of Tokyo, Tokyo 108-8639, Japan

Histone deacetylases (HDACs) are globally implicated in the growth and differentiation of mammalian cells; however, relatively little is known about their specific roles in hematopoiesis. In this study, we investigated the expression of HDACs in human hematopoietic cells and their functions during hematopoiesis. The expression of HDACs was very low in hematopoietic progenitor cells, which was accompanied by histone hyperacetylation. HDACs were detectable in more differentiated progenitors and erythroid precursors but down-regulated in mature myeloid cells especially granulocytes. In contrast, acute myeloid leukemias showed HDAC overexpression and histone hypoacetylation. Transcription of the *HDAC1* gene was repressed by CCAAT/enhancer binding proteins during myeloid differentiation, and activated by GATA-1 during erythro-megakaryocytic differentiation. Small interfering RNA-mediated knockdown of HDAC1 enhanced myeloid differentiation in immature hematopoietic cell lines and perturbed erythroid differentiation in progenitor cells. Myeloid but not erythro-megakaryocytic differentiation was blocked in mice transplanted with HDAC1-overexpressing hematopoietic progenitor cells. These findings suggest that HDAC is not merely an auxiliary factor of genetic elements but plays a direct role in the cell fate decision of hematopoietic progenitors.

Hematopoiesis is an ordered process involving self-renewal of stem cells, expansion of the lineage-committed progenitor population, and maturation into terminal elements (1). Each step is tightly regulated by several transcription factors, which confer proper expression of lineage-specific genes and/or cell cycle control genes in hematopoietic stem and progenitor cells (2). For instance, extensive biological and genetic studies indicate that GATA-1, whose expression is confined to erythroblasts, megakaryocytes, eosinophils, and mast cells, is a master regulator of erythro-megakaryocytic differentiation (3, 4), whereas GATA-2 is mainly expressed in hematopoietic stem and early progenitor cells and plays a pivotal role in self-renewal (5, 6). During myeloid differentiation, CCAAT/enhancer-binding protein (C/EBP)[3] family proteins bind to cognate sequences and transactivate a variety of myeloid-specific genes (7, 8). Although there may be some functional redundancy and overlap among C/EBPs, genetic studies reveal that *Cebpa* and *Cebpb* are essential for granulocytic differentiation and macrophage functions, respectively (8, 9).

Acute myeloblastic leukemia (AML) is characterized by deregulated proliferation and impaired differentiation of hematopoietic stem cells or immature progenitor cells (10). Recent investigations have greatly increased our understanding of the molecular basis of the biological properties of AML. Deregulated proliferation is mostly caused by aberrant activation of signal transduction pathways downstream of hematopoietic growth factor receptors. Prototype abnormalities of this type include mutations in growth factor receptors, such as FLT3 (*Fms*-like tyrosine kinase 3) and c-KIT. On the other hand, impaired differentiation is attributable to alterations of transcription factors, which result in the disruption of normal functions governing hematopoiesis. They are exemplified by fusion gene formation associated with chromosomal translocations, such as *PML/RARα* and *AML1/ETO*, and loss-of-function mutations of *CEBPA* and *AML1*. These two functionally distinct groups are termed class I and class II abnormalities, respectively (11). Accumulating genetic evidence strongly suggests that AML develops when a class I mutation confers a growth advantage to hematopoietic stem/progenitor cells in which differentiation is blocked by a class II mutation.

As described above, several lines of evidence underscore the importance of genetic elements in normal hematopoiesis and their disruptions in AML. In contrast, relatively little is known about the role of epigenetics in hematopoiesis as well as leukemogenesis. However, recent analyses of leukemic fusion proteins point to the involvement of histone deacetylases (HDACs) and the therapeutic implications. HDACs are a family of enzymes that catalyze the removal of acetyl groups from core histones, which results in chromatin compaction and transcriptional repression (12). Mammalian HDACs are divided

* This work was supported in part by the High-Tech Research Center Project for Private Universities: Matching Fund Subsidy from MEXT 2002–2006 and grants from the Vehicle Racing Commemorative Foundation and the Sankyo Foundation of Life Science (to Y. F.).

[S] The on-line version of this article (available at http://www.jbc.org) contains supplemental Tables S1 and S2 and Figs. S1–S7.

[1] Winner of the Jichi Medical School Graduate Student Award.

[2] To whom correspondence should be addressed: Division of Stem Cell Regulation, Center for Molecular Medicine, Jichi Medical University, 3311-1 Yakushiji, Shimotsuke, Tochigi 329-0498, Japan. Fax: 285-44-7501; E-mail: furuyu@jichi.ac.jp.

[3] The abbreviations used are: C/EBP, CCAAT/enhancer-binding protein; HDAC, histone deacetylase; AML, acute myeloblastic leukemia; BMMNC, bone marrow mononuclear cells; CFU-GM, colony-forming unit-granulocyte/macrophage; CFU-E, colony-forming unit-erythroid; BFU-E, burst-forming unit-erythroid; siRNA, small interfering RNA; RT, reverse transcription; GFP, green fluorescent protein; shRNA, short hairpin RNA; GAPDH, glyceraldehyde-3-phosphate dehydrogenase.

into four groups: class I (HDAC1, -2, -3, and -8), IIa (HDAC4, -5, -7, and -9), IIb (HDAC6 and -10), and IV (HDAC11). Class I HDACs are ubiquitously expressed and are generally involved in cell growth and differentiation (13), whereas class II HDACs have a more restricted pattern of expression (skeletal muscle, heart, and brain) and act in association with tissue-specific transcription factors. Leukemic fusion proteins, such as PML/RARα and AML-1/ETO, form a complex with HDACs with higher affinities than their normal counterparts and aberrantly suppress the expression of genes required for cell differentiation and growth control, leading to the transformation of hematopoietic progenitor cells (14, 15). Therefore, HDACs are considered direct targets of treatment in these cases. Indeed, a variety of small compounds that inhibit HDAC activity have been developed and tested as therapeutic agents for hematologic malignancies, including AML with fusion gene products, and solid tumors (16).

HDAC inhibitors can induce differentiation, cell cycle arrest, and apoptosis in AML cells irrespective of the presence of leukemic fusion proteins, suggesting that HDACs are generally involved in leukemogenesis via multiple mechanisms (16). These effects provide a rational backbone for the clinical application of HDAC inhibitors to AML. Intriguingly, recent clinical trials have revealed that HDAC inhibitors have only moderate hematologic toxicity (17, 18), but the underlying mechanisms are to be determined. Since these observations are biologically interesting and clinically important, their molecular basis is worth investigating. In this study, we therefore examined the expression of HDACs in human hematopoietic cells and their functions during hematopoiesis and found that the expression levels of HDACs determine the fate of hematopoietic progenitor cells.

EXPERIMENTAL PROCEDURES

Cells—Human bone marrow mononuclear cells (BMMNCs) were purchased from Cambrex BioScience (Walkersville, MD). $CD34^+$ cells were purified by positive selection with CD34 MicroBeads and MACS separation columns (Miltenyi Biotec, Gladbach, Germany). More than 95% of enriched cells were shown to be positive for CD34 and negative for lineage markers (19). $CD34^+$ BMMNCs represent early hematopoietic progenitors, since most express CD38 (data not shown). The remaining cells were used as $CD34^-$ BMMNCs after depleting lineage marker-expressing cells with a lineage cell depletion kit (Miltenyi Biotec). This fraction mainly consists of committed progenitors of multiple lineages and does not contain terminally differentiated elements, such as mature myeloid cells, erythroblasts, and lymphocytes.

Human AML cell lines, HL60, U937, and K562, were differentiated in serum-free GIT medium (Nihon Pharmaceutical, Tokyo, Japan) containing appropriate chemicals, as described previously (20, 21). Primary AML cells were obtained from patients at diagnosis by sedimentation on Ficoll-Hypaque density gradients. Informed consent was obtained from all subjects in accord with the requirements of the institutional review board. Samples were selected for the study only when they contained more than 90% leukemic cells and did not carry chromosomal translocations.

Cell Culture—For clonogenic growth assays, human $CD34^+$ BMMNCs and primary AML cells were plated at $0.5–1 \times 10^3$ cells/ml in methylcellulose medium supplemented with full cytokines (H4435, Stem Cell Technologies, Vancouver, Canada) (19). AML cell lines were cultured in methylcellulose medium supplemented with 10% fetal calf serum for 7 days. To form colony-forming unit-granulocyte/macrophage (CFU-GM) and colony-forming unit-erythroid (CFU-E), murine bone marrow cells were plated at 2.5×10^3 cells/ml in methylcellulose medium supplemented with a combination of stem cell factor, interleukin-3, and interleukin-6 (M3534) and erythropoietin alone (M3334), respectively.

Semiquantitative and Real Time Quantitative RT-PCR—Total cellular RNA was isolated from 1×10^4 cells and reverse-transcribed into cDNA using SuperScript reverse transcriptase and oligo(dT) primers (Invitrogen). We performed subsequent semiquantitative PCR, as described previously (2), and real time quantitative RT-PCR using Power SYBR Green PCR Master Mix (Applied Biosystems, Warrington, UK). Detailed information on primers, including sequences, corresponding nucleotide positions, and PCR product sizes, is shown in supplemental Table S1.

RNA Blotting—An equal amount (15 μg) of total cellular RNA was electrophoresed in 1% agarose gels containing formaldehyde and blotted onto Hybond N synthetic nylon membranes (Amersham Biosciences). The membranes were hybridized with ^{32}P-labeled probes in Rapid-hyb buffer (Amersham Biosciences).

Immunoblotting—Immunoblotting was carried out according to the standard method using the following antibodies: anti-HDAC1 (Sigma), anti-HDAC2 (MBL International, Woburn, MA), anti-HDAC3 (BD Pharmingen, San Jose, CA), and anti-β-actin (Ab-1; Oncogene Science, Uniondale, NY). We purchased site-specific antibodies against acetylated histones (H3-Lys^9, H3-Lys^{18}, H4-Lys^{12}, and H4-Lys^{16}) from Cell Signaling Technology (Beverly, MA).

Confocal Laser Microscopy—Confocal microscopic analysis was performed using anti-HDAC1 polyclonal (Sigma) and anti-CD34 monoclonal (Santa Cruz Biotechnology, Inc., Santa Cruz, CA) antibodies. We used Alexa 488-conjugated goat antibody to mouse immunoglobulin (Molecular Probes, Inc., Eugene, OR) and Cy3-conjugated goat antibody to rabbit immunoglobulin (Amersham Biosciences) as secondary antibodies.

Flow Cytometry Analysis and Fluorescence-activated Cell Sorting—Flow cytometry analysis and cell sorting were carried out with BD FACSaria (BD Biosciences) as described previously (19).

Plasmids and Transfection—Retroviral expression vector for HDAC1 was constructed by inserting full-length cDNA (provided by Dr. Stuart Schreiber, Harvard University, Boston, MA) upstream of the internal ribosome entry site-enhanced green fluorescent protein cassette of pMYs plasmid, as described previously (22). Retrovirus production was carried out by transfecting the plasmids into Plat-E packaging cells. Expression vectors for MZF-1, C/EBPα, C/EBPβ, GATA-1, GATA-2, and Sp1 were kindly provided by Drs. Robert Hromas (University of New Mexico, Albuquerque, NM), Atsushi Iwama (Department of Cellular and Molecular Medicine, Chiba University, Chiba,

Japan), and Mitsuru Nakamura (National Institute of Advanced Industrial Science and Technology, Tsukuba, Japan).

We used a lentiviral shRNA/siRNA expression vector pLentiLox3.7 for knockdown of HDAC1. Target sequences were designed to be homologous to wild-type cDNA sequences: *HDAC1* (forward), TggcaaaggcaagtattatgTTCAAGAGAcataatacttgcctttgccTTTTTTC; *HDAC1* (reverse), TCGAGAAAAAAggcaaaggcaagtattatgTCTCTTGAAcataatacttgcctttgcc. Scrambled sequences were used as controls. Lentiviruses were then added to cell suspensions in the presence of 8 μg/ml Polybrene and transduced for 24 h, as described previously (19).

Reporter Assays—We amplified the promoter regions of the *HDAC1* gene (−1170 to +397 and −73 to +397) by PCR and inserted them into pGL4.10 firefly luciferase vector (Promega, Madison, WI) to generate reporter plasmids. HEK293 cells were transfected with reporter plasmids along with pGL4.73 *Renilla* luciferase vector (Promega), which served as a positive control to determine transfection efficiencies, in the presence of test plasmids encoding *Sp1*, *GATA-1*, *GATA-2*, *MZF-1*, *CEBPA*, and *CEBPB* or empty vectors. After 48 h, firefly and *Renilla* luciferase activities were discriminately measured using the Dual-Luciferase reporter assay system (Promega).

Chromatin Immunoprecipitation Assays—We used the ChIP-IT chromatin immunoprecipitation kit (Active Motif, Carlsbad, CA) to perform chromatin immunoprecipitation assays. In brief, cells were fixed with 1% formaldehyde and sonicated to obtain chromatin suspensions. After centrifugation, supernatants were incubated with antibodies of interest in the presence of protein A-agarose beads. DNA fragments bound to the beads were purified with washing and subjected to PCR using primer pairs spanning −377 to −77 of the *HDAC1* gene.

Stem Cell Transplantation in Syngeneic Mice—Bone marrow mononuclear cells were isolated from C57BL/6 (Ly-5.1) donor mice (8–12 weeks of age). c-KIT-positive cells were isolated by CD117 MicroBeads in MACS separation columns (Miltenyi Biotec), and cultured overnight in Iscove's modified Dulbecco's medium supplemented with BIT 9500 and 50 ng/ml each of stem cell factor, FLT3 ligand, interleukin-3, and thrombopoietin. Prestimulated cells were infected with retroviruses harboring either pMYs-HDAC1 or an empty vector (mock) in 6-well dishes for 24 h (22, 23). Then $1-6 \times 10^5$ cells were injected through the tail vein into lethally irradiated (9.5 grays) C57BL/6 (Ly-5.2) recipient mice (8–12 weeks of age). Engraftment of transplanted cells was confirmed by measuring the percentages of GFP^+ and/or $Ly\text{-}5.1^+$ cells in the peripheral blood of recipients. All animal studies were approved by the Institutional Animal Ethics Committee and performed in accordance with the Guide for the Care and Use of Laboratory Animals formulated by the National Academy of Sciences.

RESULTS

Relative Resistance of Normal Human Hematopoietic Progenitors to HDAC Inhibitors—Given the relatively weak hematological toxicity reported in clinical trials (17, 18), we reasoned that normal human hematopoietic stem/progenitor cells are resistant to HDAC inhibitors. Indeed, normal human hematopoietic progenitors (CD34-positive/CD38-positive/lineage marker-negative bone marrow mononuclear cells ($CD34^+$ BMMNC)) generated more colonies in the presence of HDAC inhibitors than primary blasts from patients with AML and myeloid leukemia cell lines in clonogenic growth assays (Fig. 1). Interestingly, normal hematopoietic progenitors were more resistant to HDAC inhibitors than their differentiated offspring (CD34-negative and lineage marker-negative bone marrow mononuclear cells ($CD34^-$ BMMNC), which correspond to committed progenitors of multiple lineages).

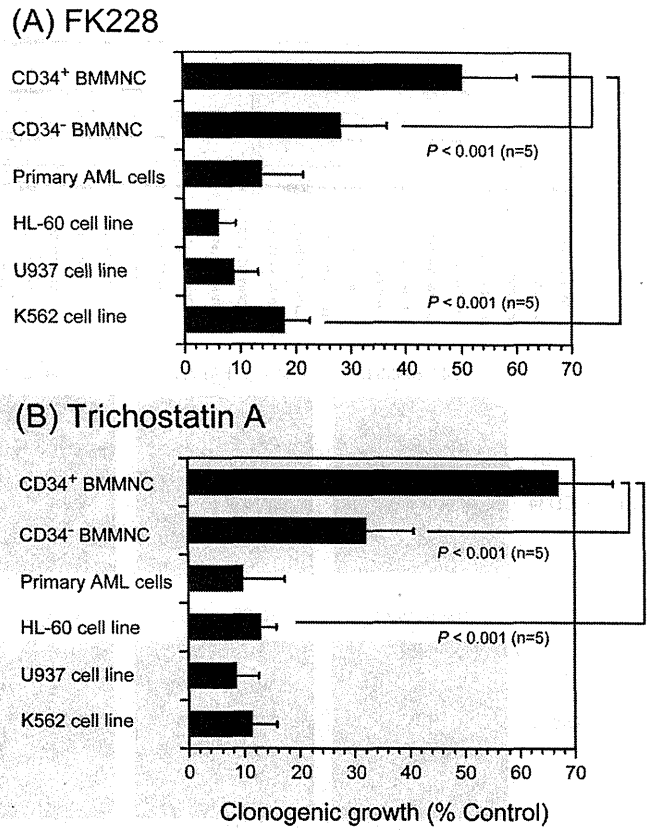

FIGURE 1. **Relative resistance of normal hematopoietic progenitor cells to HDAC inhibitors.** We seeded normal human $CD34^+$ and $CD34^-$ BMMNCs and primary AML cells at 1×10^3 cells/ml in methylcellulose medium supplemented with stem cell factor (50 ng/ml), interleukin-3 (10 ng/ml), interleukin-6 (10 ng/ml), granulocyte/macrophage colony-stimulating factor (10 ng/ml), granulocyte colony-stimulating factor (10 ng/ml), and erythropoietin (3 units/ml) and cultured in the absence or presence of either 2 nM FK228 (*A*) or 10 ng/ml trichostatin A (*B*) for 14 days. Three AML cell lines (HL-60, U937, and K562) were cultured in methylcellulose medium supplemented with 10% fetal calf serum for 7 days. Each *column* indicates the relative colony numbers setting untreated controls at 100%. The means ± S.D. (*bars*) of five independent experiments are shown. *p* values were calculated by one-way analysis of variance with the Bonferroni *post hoc* test.

Differential Expression of HDACs in Normal Hematopoietic Cells and AML Blasts—To understand the mechanisms underlying the relative resistance of normal hematopoietic progenitor cells to HDAC inhibitors, we screened for the expression of three major class I HDACs (HDAC1, -2, and -3) by immunoblotting using specific antibodies. The selection was based on the fact that these HDACs, especially HDAC1, represent the vast majority of cellular HDAC activities (13, 24) and major class II HDACs (HDAC4, -5, and -7) were scarcely expressed in hematopoietic cells in our pilot experiments (data not shown). Moreover, class I HDACs, especially HDAC1, are known to be

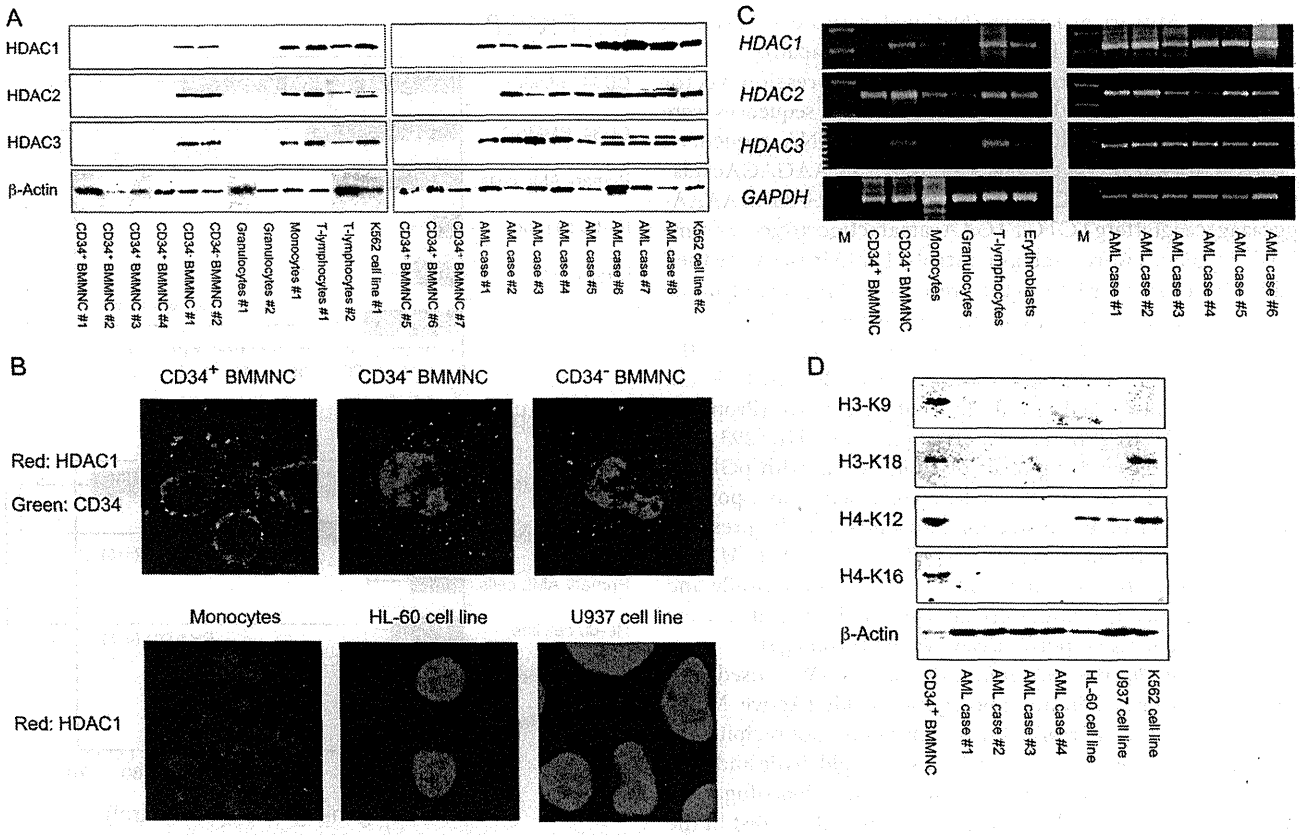

FIGURE 2. **Differential expression of HDACs in normal hematopoietic cells and AML blasts.** *A*, whole cell lysates were prepared from the indicated cell types isolated as described under "Experimental Procedures" and subjected to immunoblot analysis for the expression of HDAC1, HDAC2, HDAC3, and β-actin (loading control). Signals were obtained with the ChemiDoc XRS Molecular Imager (Bio-Rad) and used without digital manipulation except for the conversion to TIF files. See supplemental Fig. S1 for data quantification and statistical analysis. *B*, $CD34^+$ and $CD34^-$ BMNNC were stained with anti-HDAC1 (*red*) and anti-CD34 (*green*) antibodies and analyzed under confocal microscopy. Original magnification is ×600 for all *panels*. *C*, total cellular RNA was isolated from the indicated cell types, and 2.5 μg (normal hematopoietic cells) or 1.0 μg (primary AML cells) was subjected to semiquantitative RT-PCR analysis for the expression of *HDAC1*, *HDAC2*, *HDAC3*, and *GAPDH* (internal control). Five μl of the amplified products were visualized by ethidium bromide staining after 2% agarose gel electrophoresis. The results of suboptimal amplification cycles are shown: 35 and 30 cycles for *HDAC* genes and *GAPDH*, respectively. *M*, a molecular size marker (BioMarker Low; BioVentures, Inc., Murfreesboro, TN). See supplemental Fig. S3 for data quantification and statistical analysis. *D*, protein samples were analyzed by immunoblotting using specific antibodies against histone H3 acetylated at lysine 9 (*H3-K9*), histone H3 acetylated at lysine 18 (*H3-K18*), histone H4 acetylated at lysine 12 (*H4-K12*), histone H4 acetylated at lysine 16 (*H4-K16*), and β-actin (loading control). Data shown are the representative results of multiple independent experiments.

implicated in leukemogenesis and carcinogenesis and thus are pharmacological targets of most HDAC inhibitors (25, 26). As shown in Fig. 2*A*, the expression of HDAC proteins was below the detection limit in immature progenitor cells from normal human bone marrow ($CD34^+$ BMMNC). Immunoblotting with different antibodies yielded the same results, negating the possibility of the low sensitivity of the antibodies used for detection (data not shown). HDAC proteins were readily detectable in committed progenitors of multiple lineages ($Lin^-/CD34^-$ BMMNC) and T-lymphocytes but were weakly expressed in monocytes and nearly absent in mature granulocytes from the peripheral blood of healthy volunteers (see quantified data in supplemental Fig. S1). Primary leukemic cells from AML patients showed higher expression levels of HDACs than their normal counterparts (immature progenitor cells), although there was a minor case-to-case variation. In particular, HDAC1 was more abundantly expressed than HDAC2 and HDAC3 in approximately half of the cases with AML (Fig. 2*A*). We further confirmed the expression of HDAC1 using immunocytochemistry. As shown in Fig. 2*B*, HDAC1 was not detected in $CD34^+$ BMMNC, moderately expressed in the nuclei of $CD34^-$ BMMNC and monocytes, and apparently overexpressed in AML cells. The differential expression of HDACs does not simply reflect the proliferative states of these cells, because the abundance of HDACs was only modestly increased along with cell cycle entry of mitogen-stimulated T-lymphocytes (supplemental Fig. S2).

Next, we carried out similar analyses with semiquantitative RT-PCR. The expression of *HDAC* mRNAs was very weak in normal hematopoietic progenitors ($CD34^+$ BMMNC) as well as in mature myeloid cells (monocytes and granulocytes), except for *HDAC2* in $CD34^+$ BMMNC (Fig. 2*C*). *HDAC* transcripts were moderately expressed in committed progenitors ($Lin^-/CD34^-$ BMMNC), purified erythroblasts from bone marrow, and peripheral blood T-lymphocytes. In contrast, primary AML cells strongly expressed *HDAC* genes, especially *HDAC1*. The virtually identical pattern was obtained with real time quantitative RT-PCR (supplemental Fig. S3). Overall, the expression pattern of *HDAC* transcripts is nearly equal to that of HDAC proteins in normal and malignant hematopoietic

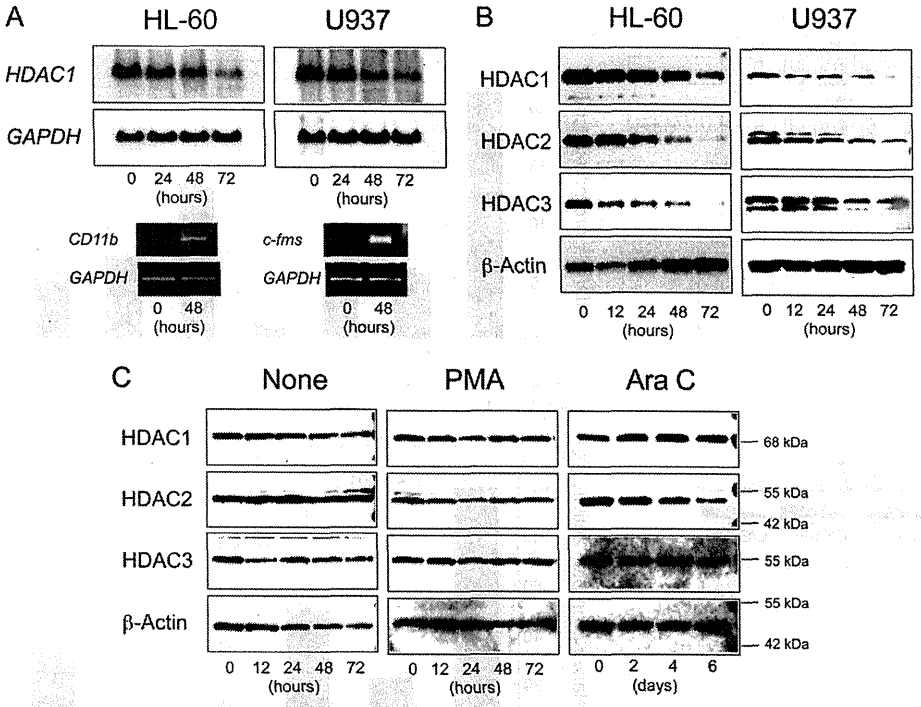

FIGURE 3. **Lineage-specific regulation of HDAC expression during hematopoietic differentiation.** HL-60 and U937 cells were cultured with all-*trans*-retinoic acid and phorbol-12-myristate-13-acetate (*PMA*) to induce granulocytic and monocytic differentiation, respectively. *A*, total cellular RNA was isolated at the indicated time points and subjected to semiquantitative RT-PCR analysis for *CD11b*, *c-fms*, and *GAPDH* (internal control) expression and Northern blot analysis for *HDAC1* and *GAPDH* expression. *B*, whole cell lysates were isolated at the indicated time points and subjected to immunoblot analysis for the expression of HDACs and β-actin (loading control). *C*, K562 cells were cultured with PMA and cytosine arabinoside (*AraC*) to induce megakaryocytic and erythroid differentiation, respectively. See supplemental Fig. S4 for the proper achievement of differentiation induction. Whole cell lysates were isolated at the indicated time points and subjected to immunoblot analysis for the expression of HDACs and β-actin (loading control). Signals were obtained with the ChemiDoc XRS Molecular Imager (Bio-Rad) and used without digital manipulation except for the conversion to TIF files. Data shown are representative results of multiple independent experiments.

cells. These results suggest that the expression of HDACs is regulated primarily at mRNA levels, but post-translational modification is also involved especially in HDAC2, as suggested by previous studies (27).

Finally, we investigated whether the acetylation status of intracellular histones reflects the distinct expression levels of HDACs in hematopoietic cells. To this end, we performed immunoblotting using site-specific antibodies against acetylated histones. As shown in Fig. 2*D*, histones H3 and H4 were heavily acetylated at Lys^9/Lys^{18} and Lys^{12}/Lys^{16}, respectively, in normal hematopoietic progenitors but not in primary AML cells. AML cell lines also lacked the acetylation of H3-Lys^9 and H4-Lys^{16}, but H4-Lys^{12} and H3-Lys^{18} were acetylated in all three cell lines examined and in K562, respectively.

Lineage-specific Regulation of HDAC Expression during Hematopoietic Differentiation—To further delineate the differential expression of HDACs in normal and malignant hematopoietic cells, we took advantage of the cell line model system. To recapitulate myeloid differentiation *in vitro*, we cultured HL-60 and U937 cells with chemical inducers of differentiation: phorbol ester, dimethyl sulfoxide, and retinoic acid (20). Successful induction of differentiation was verified by the appearance of mature myelomonocytic markers, such as *CD11b* and *c-Fms* (Fig. 3*A*, *bottom*). During myeloid differentiation, HDACs were down-regulated at both mRNA (Fig. 3*A*, *top*) and protein levels (Fig. 3*B*). We then performed similar experiments with the K562 cell line, which can be differentiated into megakaryocytic and erythroid lineages by phorbol ester and cytosine arabinoside, respectively (supplemental Fig. S4) (21). Unlike myeloid differentiation, the abundance of HDACs, especially HDAC1 and HDAC3, was unchanged during megakaryocytic and erythroid differentiation (Fig. 3*C*). Since HDAC1 seemed to be slightly increased in cytosine arabinoside-treated K562 cells, we monitored the expression of *HDAC1* during *in vitro* differentiation of primary $CD34^+$ BMMNC using real time RT-PCR. When purified $CD34^+$ BMMNCs were cultured with a combination of cytokines directing erythropoiesis (2), up-regulation of *HDAC1* expression coincided with morphological differentiation of immature progenitor cells into erythroid precursors (supplemental Fig. S5). In addition, this culture system yielded the confirmation of *HDAC1* down-regulation during myeloid differentiation of normal progenitors (data not shown).

Regulation of HDAC1 Promoter by Hematopoietic Transcription Factors—Our analyses demonstrated that HDAC expression was very low in immature hematopoietic progenitors, induced in more differentiated progenitor cells, and down-regulated during myeloid differentiation with nearly complete disappearance in mature granulocytes, whereas it was retained during erythroid and megakaryocytic differentiation. In contrast, HDACs, especially HDAC1, were overexpressed in virtually all AML cases and cell lines. To corroborate the regulatory mechanisms underlying this unique expression pattern, we isolated putative promoter regions of the *HDAC1* gene and subjected them to functional analysis. The *HDAC1* promoter contains canonical binding sites of Sp1 (GC box), MZF-1, C/EBPs (CCAAT box), and GATA transcription factors (supplemental Fig. S6). We subcloned two promoter fragments, −1179 to +397 and −73 to +397, into pGL4 luciferase vector to generate reporter plasmids as illustrated in Fig. 4*A*. The selection of analyzed regions was based on previous studies on the murine *Hdac1* promoter (28) and the results of our pilot experiments in which the segment between −1179 and +397 confers full promoter activity (data not shown). We carried out reporter assays with HEK293, because this cell line lacks the expression of transcription factors to be tested except for Sp1 (data not shown). When the −1170 construct was used, reporter assays revealed

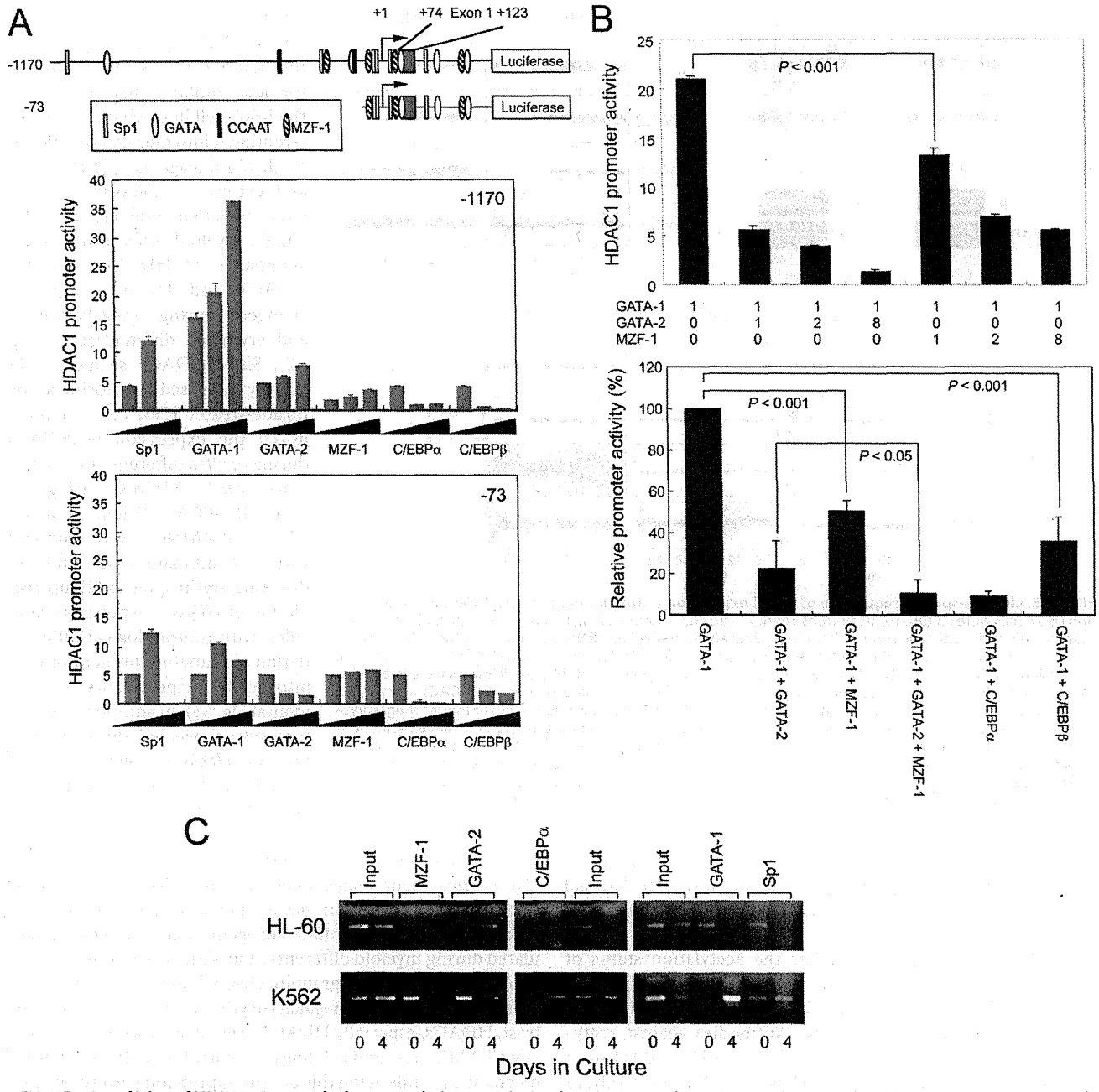

FIGURE 4. **Regulation of *HDAC1* promoter by hematopoietic transcription factors.** *A, top,* schematic representation of *HDAC1* promoter constructs used in this study. Promoter regions of the *HDAC1* gene (−1170 to +397 and −73 to +397) were linked to the luciferase gene in pGL4.10 vector as indicated. Relative locations of the putative binding sites of hematopoietic transcription factors are approximated by the *symbols* shown in the *box*. See supplemental Fig. S6 for the nucleotide sequence. *Bottom,* we transfected pGL4.10 plasmid containing *HDAC1* promoter sequences between −1170 and +397 (*−1170*) or between −73 and +397 (*−73*) into HEK293 cells along with expression vectors encoding *Sp1, GATA-1, GATA-2, MZF-1, CEBPA,* and *CEBPB* at various doses (1, 2, and 4 μg) and measured luciferase activities after 48 h. *HDAC1* promoter activity (*y* axis) was calculated as firefly luciferase activities of cells transfected with either pGL4.10−1170 or pGL4.10−73 and an empty expression vector setting at 1.0 after normalization of transfection efficiencies using *Renilla* luciferase activity. Data shown are the means ± S.D. of three independent experiments. *B, top,* we transfected pGL4.10−1170 reporter plasmid into HEK293 cells along with expression vectors encoding *GATA-1, GATA-2,* and *MZF-1* at the indicated doses (μg) and measured luciferase activity after 48 h. HDAC1 promoter activity (*y* axis) was calculated as firefly luciferase activities of cells transfected with pGL4.10−1170 and an empty expression vector set at 1.0 after normalization of transfection efficiencies using Renilla luciferase activities. *Bottom,* we transfected pGL4.10−1170 reporter plasmid and 1 μg of *GATA-1* expression vector into HEK293 cells in the absence or presence of 1 μg of expression plasmids encoding *GATA-2, MZF-1, CEBPα,* and *CEBPβ* and measured luciferase activities after 48 h. Relative promoter activity (*y* axis) was calculated as firefly luciferase activities of cells transfected with pGL4.10−1170 and *GATA-1* expression vector setting at 100% after normalization of transfection efficiencies using *Renilla* luciferase activities. Data shown are the means ± S.D. of three independent experiments. *p* values were calculated by one-way analysis of variance with the Student-Newman-Keuls multiple comparisons test. *C,* HL60 and K562 were cultured in the presence of PMA for 4 days and harvested before and after differentiation for chromatin immunoprecipitation assays. Chromatin suspensions were immunoprecipitated with the indicated antibodies and corresponding control antibodies. The resulting precipitants were subjected to PCR to amplify the promoter region (−377 to −77) of the *HDAC1* gene. The amplified products were visualized by ethidium bromide staining after 2% agarose gel electrophoresis. Representative data of 50 cycles are shown. *Input,* PCR was performed with genomic DNA.

that *HDAC1* transactivation was driven by Sp1 and GATA-1 (Fig. 4*A*, *middle*). In contrast, members of the C/EBP family transcription factors, C/EBPα and C/EBPβ, negatively regulated transcription of the *HDAC1* gene. GATA-2 and MZF-1 showed only a modest effect on promoter activity. Sp1 was able to activate the −73 construct to a similar extent as the −1170 construct, suggesting that GC boxes surrounding the transcription start site are responsible for Sp1-mediated transactivation of *HDAC1* (Fig. 4*A*, *bottom*). However, the activity of GATA-1 was significantly diminished when the −73 construct was used, implying that consensus sequences at the positions −973 and −91 are necessary for GATA-1 to fully activate the *HDAC1* promoter. In contrast, C/EBPα and C/EBPβ were still able to repress the *HDAC1* promoter in the −73 construct. Since the −73 construct lacks CCAAT boxes, the suppressor function of C/EBPs may be mediated via interaction with activator proteins, most likely GATA-1 (7, 29). To verify this hypothesis, we examined the effects of C/EBPα and C/EBPβ on GATA-1-mediated transactivation of the *HDAC1* gene using co-transfection. As anticipated, both C/EBPα and C/EBPβ significantly suppressed *HDAC1* promoter activation by GATA-1. In particular, C/EBPα suppressed the activity of GATA-1 to about one-tenth (Fig. 4*B*, *bottom*). More importantly, GATA-2 and MZF-1 individually antagonized GATA-1-mediated activation of the *HDAC1* promoter in a dose-dependent manner (Fig. 4*B*, *top*), and the two factors synergistically suppressed it (Fig. 4*B*, *bottom*).

Next, we investigated the binding of these factors to *HDAC1* promoter *in vivo* and its changes during hematopoietic differentiation using chromatin immunoprecipitation assays. In an undifferentiated HL-60 cell line, Sp1 and GATA-1 bound to the sequence between −377 and −77, which was shown to be the active regulatory region by reporter assays (Fig. 4*C*, day 0). This suggests that these two factors confer the base-line expression of *HDAC1* in the myeloid-committed cell line HL-60. Upon differentiation, both Sp1 and GATA-1 dissociated from the *HDAC1* promoter, and GATA-2 and a small amount of C/EBPα became detectable (Fig. 4*C*, day 4). These results suggest that the exchange of positive to negative regulators on the promoter contributes to the silencing of *HDAC1* during myeloid differentiation. On the other hand, the binding of Sp1, MZF-1, and GATA-2 was demonstrated in an untreated K562 cell line, whereas GATA-1 binding was not observed (Fig. 4*C*, day 0). The difference of binding factors may be attributed to the fact that K562 is more immature than HL-60 and possesses pluripotency (21). Sp1 and GATA-2 may render the base-line expression of *HDAC1* in K562 cells, because GATA-2 appears to be a weak activator in the absence of GATA-1 in reporter assays. Upon megakaryocytic differentiation, the strongest activator GATA-1 was recruited to the promoter along with the dissociation of its inhibitors MZF-1 and GATA-2 in K562 cells. In addition, there was a slight increase in the binding of Sp1 (Fig. 4*C*, day 4). These changes may underlie the sustained expression of *HDAC1* during megakaryocytic differentiation.

Expression Levels of HDAC1 Affect the Differentiation Program of Hematopoietic Progenitor Cells—One important question regarding the expression pattern of HDACs during differentiation is whether the change is a simple consequence of differentiation or if it has a functional meaning. To address this question, we carried out loss-of-function studies using siRNA against HDAC1, which represents more than half of HDAC activities in mammalian cells and cannot be compensated by other class I HDACs (13, 24). In a myeloid-committed cell line HL-60, siRNA-mediated knockdown of HDAC1 promoted myeloid differentiation, as revealed by a decrease in the expression of CD33, a marker of immature myeloid cells (30) (Fig. 5*A*). This suggests that HDAC1 is indispensable for the maintenance of an immature state in HL-60 cells. In multipotent K562 cells, the suppression of HDAC1 caused a decrease of an erythroid marker CD235a and a reciprocal increase of a mature myeloid marker CD11b (Fig. 5*B*). This implies that overexpressed HDAC1 maintains the erythroid properties of K562 cells, and its reduction results in retrograde differentiation into a myeloid lineage. This is compatible with the expression pattern of HDACs in hematopoietic cells. In addition, we examined the effects of HDAC1 knockdown on normal progenitor cells in clonogenic assays. $CD34^+$ human BMMNCs were transduced with siRNA expression vectors and cultured in methylcellulose medium with full cytokines to induce both myeloid and erythroid differentiation. HDAC1 knockdown reduced the numbers and sizes of erythroid colonies, CFU-E and burst-forming unit-erythroid (BFU-E), with a reciprocal increase in granulocyte/macrophage colonies (Fig. 5*C*). Taken together, these results point to an instructive role of HDACs in lineage specification during hematopoiesis.

HDAC1 Overexpression Blocks Myeloid Differentiation in a Murine Stem Cell Transplantation Model—The data so far suggest that HDAC expression should be repressed in normal hematopoietic progenitors, and HDAC overexpression alters the differentiation program, leading to myeloid leukemogenesis. To investigate whether HDAC overexpression actually results in the deregulation of hematopoietic differentiation, we performed stem cell transplantation studies in syngeneic mice (22, 23). We isolated c-KIT-positive bone marrow mononuclear cells from C57BL/6 (Ly-5.1) mice and infected them with retroviruses carrying either *HDAC1* cDNA with green fluorescent protein (GFP) or GFP alone (mock). The validity of the expression vector was confirmed by checking HDAC1 overexpression and target gene silencing in transfected cells (supplemental Fig. S7). We transplanted HDAC1- or mock-transfected cells into a lethally irradiated C57BL/6 (Ly-5.2) strain and monitored engraftment by measuring the percentages of GFP-positive and/or Ly-5.1- positive cells in peripheral blood serially. As shown in Fig. 6*A*, both HDAC1- and mock-transfected progenitor cells successfully reconstructed hematopoiesis in recipient mice 4 weeks after transplantation. However, donor-derived leukocytes gradually declined in the peripheral blood of mice that received HDAC1-transduced cells after 12 weeks and became nearly undetectable after 28 weeks (Fig. 6*A*). In contrast, there were no significant changes in the numbers of red blood cells and platelets between HDAC1- and mock-transplanted mice (data not shown). This is in line with the results of our *in vitro* studies indicating that HDAC expression is required for erythro-megakaryocytic differentiation. Leukemic transformation of transplanted cells was not observed up to 60 weeks after transplantation.

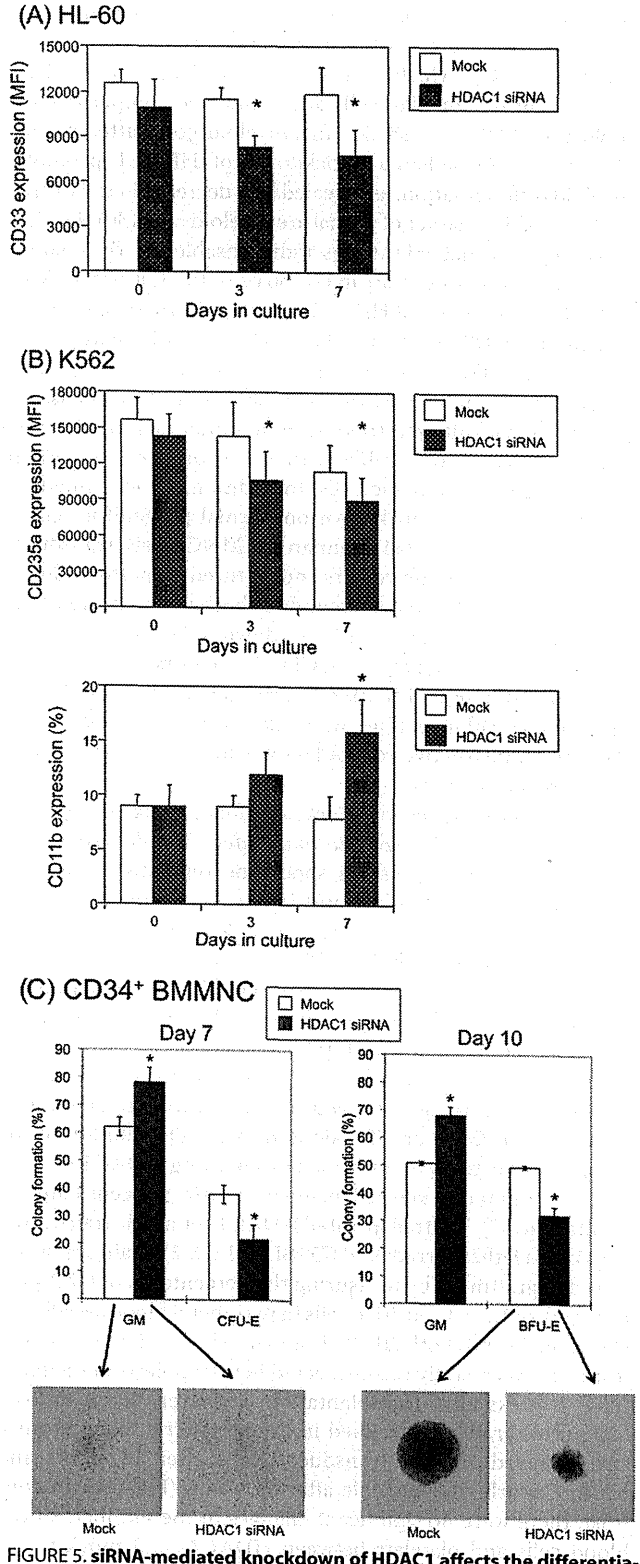

FIGURE 5. **siRNA-mediated knockdown of HDAC1 affects the differentiation program of hematopoietic progenitor cells.** *A*, HL-60 cells were transfected with lentivirus vectors carrying shRNA/siRNA against scrambled sequences (*Mock*) or *HDAC1* (*HDAC1 siRNA*) and subjected to flow cytometric analysis at the indicated time points. Data shown are the means ± S.D. (*bars*) of the mean fluorescence intensity (*MFI*) of CD33 in GFP-positive fractions ($n = 3$). p values were calculated by paired Student's t test (*, $p < 0.05$). *B*, K562 cells were transfected with lentiviral vectors carrying shRNA/siRNA against scrambled sequences or *HDAC1* and subjected to flow cytometric analysis at the indicated time points. Data shown are the means ± S.D. (*bars*) of the mean fluorescence intensity of CD235a and a percentage of CD11b-positive cells in GFP-positive fractions ($n = 3$). p values were calculated by paired Student's t test (*, $p < 0.05$). *C*, CD34$^+$ human bone marrow mononuclear cells were transfected with lentivirus vectors carrying shRNA/siRNA against scrambled sequences or *HDAC1*. GFP-positive cells were sorted and seeded at 0.5–1 × 10^3 cells/ml in methylcellulose medium supplemented with full cytokines as described in the legend to Fig. 1. The numbers of CFU-GM/CFU-E and CFU-GM/BFU-E were counted after 7 and 10 days of culture, respectively, and expressed as relative percentages. Data shown are the means ± S.D. of three independent experiments. p values were calculated by paired Student's t test (*, $p < 0.05$). Representative photographs are shown *below* (original magnification, ×100).

Next, we analyzed the components of bone marrow 10 weeks after transplantation. In HDAC1-transduced mice, there was a significant reduction of c-KIT-positive progenitors and CD11b-positive myeloid cells, whereas CD3- and B220-positive lymphoid cells were relatively increased compared with mock-transfected mice (Fig. 6*B*). Consistent with normal numbers of red blood cells and platelets in peripheral blood, immature cells of both lineages were normal or slightly increased in the bone marrow of HDAC1-transduced mice. These results indicate that HDAC1 exclusively perturbs myelopoiesis when overexpressed in hematopoietic progenitor cells. To corroborate this notion, we isolated c-KIT/GFP double-positive cells from bone marrow of mice transplanted with either HDAC1- or mock-transduced progenitors and subjected them to *in vitro* clonogenic growth assays. As shown in Fig. 6*C*, HDAC1 overexpression reduced the formation of CFU-GM, which corresponds to committed progenitors of myeloid lineage, without affecting mature erythroid progenitors CFU-E. HDAC1-transduced progenitors did not produce spontaneous colonies in this assay (Fig. 6*C*, *No CSF*). Furthermore, replating experiments yielded few or no secondary and tertiary colonies in semisolid medium even in the presence of growth factors (data not shown). These results suggest that HDAC1 overexpression alone cannot immortalize hematopoietic stem/progenitor cells, which is in line with the observation of transplantation studies.

DISCUSSION

Class I histone deacetylases are globally implicated in the growth and differentiation of mammalian cells by modifying chromatin structures and gene expression (12, 13). However, relatively little is known about their specific roles in normal hematopoiesis. In this study, we investigated the expression and function of major class I HDACs in normal human hematopoietic cells and obtained the following novel findings. First, the expression of HDACs is very low in CD34$^+$ hematopoietic progenitor cells. Second, HDAC1 plays an instructive role in lineage specification during hematopoiesis. Finally, HDAC1 is overexpressed in AML cells and contributes to leukemogenesis by perturbing myeloid differentiation. Overall, these findings indicate that HDAC is not merely an auxiliary factor of genetic elements but plays a direct role in the cell fate decision of hematopoietic progenitors.

The biological significance of the low level expression of HDACs in hematopoietic progenitor cells has yet to be determined; however, this phenomenon explains why hematological

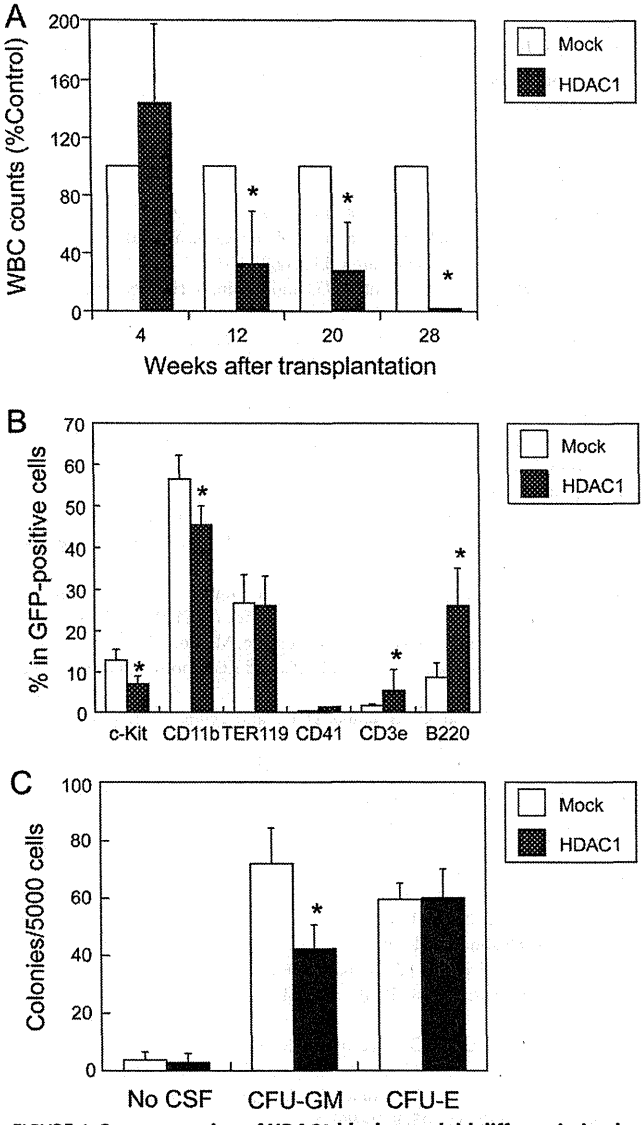

FIGURE 6. **Overexpression of HDAC1 blocks myeloid differentiation in a murine stem cell transplantation model.** Purified c-KIT-positive bone marrow cells from C57BL/6 (Ly-5.1) mice were transfected with retroviruses carrying either GFP alone (*Mock*) or HDAC1/GFP (*HDAC1*) and transplanted into lethally irradiated C57BL/6 (Ly-5.2) mice. *A*, peripheral blood was drawn at the indicated time points and subjected to blood counting. The numbers of white blood cells are shown as percentages of those of mock-transplanted mice. *B*, bone marrow mononuclear cells were subjected to flow cytometric analysis of surface marker expression. Data shown are the means ± S.D. (*bars*) of percentages of each surface marker in GFP-positive fractions ($n = 3$). *C*, GFP-positive bone marrow mononuclear cells were cultured in semisolid culture medium supplemented with appropriate cytokines as described under "Experimental Procedures." Colony numbers were counted after 14 days. Data shown are the means ± S.D. of three independent experiments. *p* values were calculated by paired Student's *t* test (*, $p < 0.05$).

toxicity is relatively weak in patients treated with HDAC inhibitors (17, 18). Inoue *et al.* (31) have also reported that the expression of *Hdac1* mRNA is extremely low in purified murine hematopoietic stem cells compared with cumulus and other somatic cells. They speculate that low HDAC activity underlies insufficient reprogramming of the genome from hematopoietic stem cells after nuclear transfer, which is consistent with the general consensus that hematopoiesis is difficult to reconstruct *in vitro* by genetic manipulation (32). Our findings fully support their view and further suggest that hematopoietic stem/progenitor cells may possess a unique genetic program, which characterizes the hematopoietic system.

Accumulating evidence indicates that hematopoietic stem/progenitor cells express a wide variety of genes required for multiple differentiation programs, most of which become repressed as lineage choices are restricted during terminal differentiation (33–35). This "priming" of multiple genes is considered to be essential for hematopoietic stem/progenitor cells to maintain multipotency. To accomplish this unique property, hematopoietic stem/progenitor cells have an open chromatin state, which is achieved by hyperacetylation of promoter histones. The low abundance of HDACs should contribute to histone hyperacetylation of "primed" genes in hematopoietic stem/progenitor cells. Indeed, multiple sites of core histones were hyperacetylated in $CD34^+$ progenitor cells compared with AML cells in our study. Moreover, up-regulation of HDACs in more differentiated/committed progenitors is consistent with this notion. If this scenario is true, exogenous interference with the up-regulation of HDACs may inhibit the differentiation of progenitor cells, leading to their expansion. Recent investigations suggest that this is the case: pharmacological down-regulation of HDACs effectively expands hematopoietic progenitor cells *ex vivo* (36, 37). Similarly, Haumaitre *et al.* (38) succeeded in amplifying endocrine progenitor cells using HDAC inhibitors.

In this study, we also found that HDAC1 has an instructive role in lineage specification of human hematopoietic cells. *HDAC1* is up-regulated in differentiating progenitor cells of multiple lineages by down-regulation of GATA-2 and MZF-1, which are abundantly expressed in early progenitor cells (39, 40). Common myeloid progenitors differentiate into erythro-megakaryocytic lineages when *HDAC1* expression is sustained by GATA-1. In contrast, they differentiate into myeloid cells, especially granulocytes, when *HDAC1* is down-regulated by C/EBPs. This view is compatible with the recent report by Yamamura *et al.* (41), in which pharmacological inhibition of HDAC activities enhances interleukin-3 and stem cell factor-mediated generation of committed progenitors from human peripheral blood-derived $CD34^+$ cells and inhibits erythropoietin-induced erythroid differentiation of committed progenitors. Furthermore, experiments using HDAC inhibitors have revealed the roles of HDACs in the differentiation of several cell types, including neurons, oligodendrocytes, osteoblasts, intestinal epithelial cells, adipocytes, and regulatory T cells (42–44). Our results provide the molecular basis of these observations and the rationale for medical application of HDAC inhibitors to tissue regeneration.

Finally, we found that HDACs are overexpressed in nearly all primary AML cells and cell lines without fusion gene products caused by chromosomal translocations. The involvement of HDACs in leukemogenesis in AML cells carrying fusion gene products has been well characterized and provides a theoretical basis for the efficacy of HDAC inhibitors for acute leukemias with chromosomal translocations (14, 15). Our findings extend this view and propose more generalized roles of HDACs in leukemogenesis and the validity of class I HDACs as therapeutic

targets in various hematological malignancies. As a result of HDAC overexpression, histone acetylation was diminished at multiple residues, including histone H4-lysine 16. Loss of acetylation at histone H4-lysine 16 was shown to be an epigenetic hallmark of human cancer, including AML, by Fraga *et al.* (45). Therefore, overexpression of HDACs may be a common feature of malignant cells, playing a fundamental role in oncogenesis. Indeed, overexpression of HDACs, mostly HDAC1, has been described in gastric, prostate, breast, cervical, and colon cancers (46, 47). As for the mechanisms of HDAC overexpression in AML, we speculate that loss-of-function mutations of C/EBP or abnormalities in the expression of MZF-1 and GATA2 cause aberrant expression of *HDAC1* in hematopoietic stem/progenitor cells. Although further investigation is required to elucidate the underlying mechanisms, HDAC overexpression justifies the application of HDAC inhibitors for cancer treatment.

According to the two-hit theory, two independent genetic abnormalities are required for the development of AML (11). Class I mutations confer a growth advantage on hematopoietic stem cells, and class II mutations block differentiation. The results of our transplantation studies suggest that *HDAC1* acts as a novel class II transforming gene upon overexpression in hematopoietic stem/progenitor cells. From a mechanistic standpoint, two questions emerge immediately. What is the identity of the downstream effectors? What are the accompanying class I mutations? To address the first question, we performed DNA microarray analysis of HDAC1-transduced c-KIT-positive bone marrow cells from recipient mice. Among 22,201 genes screened, the expressions of 153 genes (0.69%) were up-regulated more than 2-fold in HDAC1-transduced c-KIT$^+$ progenitor cells compared with mock-transfected control (supplemental Fig. S8). Similarly, down-regulation was observed in 63 genes (0.28%). Supplemental Table S2 shows part of the HDAC1-regulated genes, in which the alteration of the expression levels was confirmed by real time quantitative RT-PCR. Among them, up-regulation of c-*Mpl* is most interesting, because it is essential for megakaryocyte development (48) and for maintaining hematopoietic stem cells in the G_0 phase of the cell cycle (49). It is possible that up-regulated c-MPL directs HDAC1-expressing progenitors into quiescence and also skews their differentiation program into erythro-megakaryocytic lineage. Regarding the second question, we have found a positive correlation of the presence of internal tandem duplication of FLT3 (FLT3-ITD), the most frequent class I abnormality in *de novo* AML (50), with the expression levels of HDAC1 (supplemental Fig. S9). This strongly suggests that HDAC1 overexpression and FLT3 mutations collaborate to transform progenitor cells into leukemic clones. Extensive investigation is currently under way in our laboratory to address the functional interplay between HDAC1 overexpression and c-MPL up-regulation and/or FLT3 mutations in leukemogenesis.

In summary, our findings add new insight into the epigenetic regulation of normal and malignant hematopoiesis and ultimately contribute to the development of better treatment strategies in diseases of the hematopoietic system.

Acknowledgments—We are grateful to Dr. Tsukasa Ohmori (Jichi Medical School) for helpful discussions and technical advice and Drs. Stuart Schreiber, Robert Hromas, Atsushi Iwama, and Mitsuru Nakamura for materials.

REFERENCES

1. Orkin, S. H., and Zon, L. I. (2008) *Cell* **132,** 631–644
2. Furukawa, Y., Kikuchi, J., Nakamura, M., Iwase, S., Yamada, H., and Matsuda, M. (2000) *Br. J. Haematol.* **110,** 663–673
3. Martin, D. I., Zon, L. I., Mutter, G., and Orkin, S. H. (1990) *Nature* **344,** 444–447
4. Orkin, S. H., Shivdasani, R. A., Fujiwara, Y., and Mcdevitt, M. A. (1998) *Stem Cells* **16,** 79–83
5. Heyworth, C., Gale, K., Dexter, M., May, G., and Enver, T. (1999) *Genes Dev.* **13,** 1847–1860
6. Ling, K. W., Ottersbach, K., van Hamburg, J. P., Oziemlak, A., Tsai, F. Y., Orkin, S. H., Ploemacher, R., Hendriks, R. W., and Dzierzak, E. (2004) *J. Exp. Med.* **200,** 871–882
7. Iwasaki, H., Mizuno, S., Arinobu, Y., Ozawa, H., Mori, Y., Shigematsu, H., Takatsu, K., Tenen, D. G., and Akashi, K. (2006) *Genes Dev.* **20,** 3010–3021
8. Zhang, D. E., Zhang, P., Wang, N. D., Hetherington, C. J., Darlington, G. J., and Tenen, D. G. (1997) *Proc. Natl. Acad. Sci. U.S.A.* **94,** 569–574
9. Tanaka, T., Akira, S., Yoshida, K., Umemoto, M., Yoneda, Y., Shirafuji, N., Fujiwara, H., Suematsu, S., Yoshida, N., and Kishimoto, T. (1995) *Cell* **27,** 353–361
10. Fröhling, S., Scholl, C., Gilliland, D. G., and Levine, R. L. (2005) *J. Clin. Oncol.* **23,** 6285–6295
11. Gilliland, D. G. (2002) *Semin. Hematol.* **39,** 6–11
12. Yang, X. J., and Seto, E. (2008) *Nat. Rev. Mol. Cell Biol.* **9,** 206–218
13. Lagger, G., O'Carroll, D., Rembold, M., Khier, H., Tischler, J., Weitzer, G., Schuettengruber, B., Hauser, C., Brunmeir, R., Jenuwein, T., and Seiser, C. (2002) *EMBO J.* **21,** 2672–2681
14. Lin, R. J., Nagy, L., Inoue, S., Shao, W., Miller, W. H., Jr., and Evans, R. M. (1998) *Nature* **391,** 811–814
15. Wang, J., Hoshino, T., Redner, R. L., Kajigaya, S., and Liu, J. M. (1998) *Proc. Natl. Acad. Sci. U.S.A.* **95,** 10860–10865
16. Xu, W. S., Parmigiani, R. B., and Marks, P. A. (2007) *Oncogene* **26,** 5541–5552
17. Byrd, J. C., Marcucci, G., Parthun, M. R., Xiao, J. J., Klisovic, R. B., Moran, M., Lin, T. S., Liu, S., Sklenar, A. R., Davis, M. E., Lucas, D. M., Fischer, B., Shank, R., Tejaswi, S. L., Binkley, P., Wright, J., Chan, K. K., and Grever, M. R. (2005) *Blood* **105,** 959–967
18. O'Connor, O. A., Heaney, M. L., Schwartz, L., Richardson, S., Willim, R., MacGregor-Cortelli, B., Curly, T., Moskowitz, C., Portlock, C., Horwitz, S., Zelenetz, A. D., Frankel, S., Richon, V., Marks, P., and Kelly, W. K. (2006) *J. Clin. Oncol.* **24,** 166–173
19. Kikuchi, J., Shimizu, R., Wada, T., Ando, H., Nakamura, M., Ozawa, K., and Furukawa, Y. (2007) *Stem Cells* **25,** 2439–2447
20. Zhao, K. W., Li, X., Zhao, Q., Huang, Y., Li, D., Peng, Z. G., Shen, W. Z., Zhao, J., Zhou, Q., Chen, Z., Sims, P. J., Wiedmer, T., and Chen, G. Q. (2004) *Blood* **104,** 3731–3738
21. Terui, Y., Furukawa, Y., Kikuchi, J., Iwase, S., Hatake, K., and Miura, Y. (1998) *Exp. Hematol.* **26,** 236–244
22. Kitamura, T., Koshino, Y., Shibata, F., Oki, T., Nakajima, H., Nosaka, T., and Kumagai, H. (2003) *Exp. Hematol.* **31,** 1007–1014
23. Ono, R., Nakajima, H., Ozaki, K., Kumagai, H., Kawashima, T., Taki, T., Kitamura, T., Hayashi, Y., and Nosaka, T. (2005) *J. Clin. Invest.* **115,** 919–929
24. Li, J., Lin, Q., Wang, W., Wade, P., and Wong, J. (2002) *Genes Dev.* **16,** 687–692
25. Senese, S., Zaragoza, K., Minardi, S., Muradore, I., Ronzoni, S., Passafaro, A., Bernard, L., Draetta, G. F., Alcalay, M., Seiser, C., and Chiocca, S. (2007) *Mol. Cell Biol.* **27,** 4784–4795
26. Glozak, M. A., and Seto, E. (2007) *Oncogene* **26,** 5420–5432
27. Krämer, O. H., Zhu, P., Ostendorff, H. P., Golebiewski, M., Tiefenbach, J.,

Peters, M. A., Brill, B., Groner, B., Bach, I., Heinzel, T., and Göttlicher, M. (2003) *EMBO J.* **22,** 3411–3420
28. Schuettengruber, B., Simboeck, E., Khier, H., and Seiser, C. (2003) *Mol. Cell Biol.* **23,** 6993–7004
29. Tong, Q., Tsai, J., Tan, G., Dalgin, G., and Hotamisligil, G. S. (2005) *Mol. Cell Biol.* **25,** 706–715
30. Stelzer, G. T., Shults, K. E., and Loken, M. R. (1993) *Ann. N.Y. Acad. Sci.* **677,** 265–280
31. Inoue, K., Ogonuki, N., Miki, H., Hirose, M., Noda, S., Kim, J. M., Aoki, F., Miyoshi, H., and Ogura, A. (2006) *J. Cell Sci.* **119,** 1985–1991
32. Ledran, M. H., Krassowska, A., Armstrong, L., Dimmick, I., Renström, J., Lang, R., Yung, S., Santibanez-Coref, M., Dzierzak, E., Stojkovic, M., Oostendorp, R. A., Forrester, L., and Lako, M. (2008) *Cell Stem Cell* **3,** 85–98
33. Hu, M., Krause, D., Greaves, M., Sharkis, S., Dexter, M., Heyworth, C., and Enver, T. (1997) *Genes Dev.* **11,** 774–785
34. Warren, L., Bryder, D., Weissman, I. L., and Quake, S. R. (2006) *Proc. Natl. Acad. Sci. U.S.A.* **103,** 17807–17812
35. Azuara, V., Perry, P., Sauer, S., Spivakov, M., Jørgensen, H. F., John, R. M., Gouti, M., Casanova, M., Warnes, G., Merkenschlager, M., and Fisher, A. G. (2006) *Nat. Cell Biol.* **8,** 532–538
36. De Felice, L., Tatarelli, C., Mascolo, M. G., Gregorj, C., Agostini, F., Fiorini, R., Gelmetti, V., Pascale, S., Padula, F., Petrucci, M. T., Arcese, W., and Nervi, C. (2005) *Cancer Res.* **65,** 1505–1513
37. Bug, G., Gül, H., Schwarz, K., Pfeifer, H., Kampfmann, M., Zheng, X., Beissert, T., Boehrer, S., Hoelzer, D., Ottmann, O. G., and Ruthardt, M. (2005) *Cancer Res.* **65,** 2537–2541
38. Haumaitre, C., Lenoir, O., and Scharfmann, R. (2008) *Mol. Cell Biol.* **28,** 6373–6383
39. Nagai, T., Harigae, H., Ishihara, H., Motohashi, H., Minegishi, N., Tsuchiya, S., Hayashi, N., Gu, L., Andres, B., Engel, J. D., and Yamamoto, M. (1994) *Blood* **84,** 1074–1084
40. Gaboli, M., Kotsi, P. A., Gurrieri, C., Cattoretti, G., Ronchetti, S., Cordon-Cardo, C., Broxmeyer, H. E., Hromas, R., and Pandolfi, P. P. (2001) *Genes Dev.* **15,** 1625–1630
41. Yamamura, K., Ohishi, K., Katayama, N., Yu, Z., Kato, K., Masuya, M., Fujieda, A., Sugimoto, Y., Miyata, E., Shibasaki, T., Heike, Y., Takaue, Y., and Shiku, H. (2006) *Br. J. Haematol.* **135,** 242–253
42. Hsieh, J., Nakashima, K., Kuwabara, T., Mejia, E., and Gage, F. H. (2004) *Proc. Natl. Acad. Sci. U.S.A.* **101,** 16659–16664
43. Shen, S., Sandoval, J., Swiss, V. A., Li, J., Dupree, J., Franklin, R. J., and Casaccia-Bonnefil, P. (2008) *Nat. Neurosci.* **11,** 1024–1034
44. Tao, R., de Zoeten, E. F., Ozkaynak, E., Chen, C., Wang, L., Porrett, P. M., Li, B., Turka, L. A., Olson, E. N., Greene, M. I., Wells, A. D., and Hancock, W. W. (2007) *Nat. Med.* **13,** 1299–1307
45. Fraga, M. F., Ballestar, E., Villar-Garea, A., Boix-Chornet, M., Espada, J., Schotta, G., Bonaldi, T., Haydon, C., Ropero, S., Petrie, K., Iyer, N. G., Pérez-Rosado, A., Calvo, E., Lopez, J. A., Cano, A., Calasanz, M. J., Colomer, D., Piris, M. A., Ahn, N., Imhof, A., Caldas, C., Jenuwein, T., and Esteller, M. (2005) *Nat. Genet.* **37,** 391–400
46. Zhang, Z., Yamashita, H., Toyama, T., Sugiura, H., Ando, Y., Mita, K., Hamaguchi, M., Hara, Y., Kobayashi, S., and Iwase, H. (2005) *Breast Cancer Res. Treat.* **94,** 11–16
47. Zhu, P., Martin, E., Mengwasser, J., Schlag, P., Janssen, K. P., and Göttlicher, M. (2004) *Cancer Cell* **5,** 455–463
48. Gurney, A. L., Carver-Moore, K., de Sauvage, F. J., and Moore, M. W. (1994) *Science* **265,** 1445–1447
49. Yoshihara, H., Arai, F., Hosokawa, K., Hagiwara, T., Takubo, K., Nakamura, Y., Gomei, Y., Iwasaki, H., Matsuoka, S., Miyamoto, K., Miyazaki, H., Takahashi, T., and Suda, T. (2007) *Cell Stem Cell* **1,** 685–697
50. Parcells, B. W., Ikeda, A. K., Simms-Waldrip, T., Moore, T. B., and Sakamoto, K. M. (2006) *Stem Cells* **24,** 1174–1184

Identity of the elusive IgM Fc receptor (FcμR) in humans

Hiromi Kubagawa,[1] Satoshi Oka,[1] Yoshiki Kubagawa,[1] Ikuko Torii,[1] Eiji Takayama,[1] Dong-Won Kang,[1] G. Larry Gartland,[2] Luigi F. Bertoli,[3] Hiromi Mori,[4] Hiroyuki Takatsu,[4] Toshio Kitamura,[5] Hiroshi Ohno,[4] and Ji-Yang Wang[4]

[1]Department of Pathology and [2]Department of Medicine, University of Alabama at Birmingham, Birmingham, AL 35294
[3]Brookwood Medical Center, Birmingham, AL 35294
[4]RIKEN Research Center for Allergy and Immunology, Tsurumi, Yokohama 230-0045, Japan
[5]Institute of Medical Science, University of Tokyo, Minato-ku, Tokyo 108-8639, Japan

Although Fc receptors (FcRs) for switched immunoglobulin (Ig) isotypes have been extensively characterized, FcR for IgM (FcμR) has defied identification. By retroviral expression and functional cloning, we have identified a complementary DNA (cDNA) encoding a bona fide FcμR in human B-lineage cDNA libraries. FcμR is defined as a transmembrane sialoglycoprotein of ~60 kD, which contains an extracellular Ig-like domain homologous to two other IgM-binding receptors (polymeric Ig receptor and Fcα/μR) but exhibits an exclusive Fcμ-binding specificity. The cytoplasmic tail of FcμR contains conserved Ser and Tyr residues, but none of the Tyr residues match the immunoreceptor tyrosine-based activation, inhibitory, or switch motifs. Unlike other FcRs, the major cell types expressing FcμR are adaptive immune cells, including B and T lymphocytes. After antigen-receptor ligation or phorbol myristate acetate stimulation, FcμR expression was up-regulated on B cells but was down-modulated on T cells, suggesting differential regulation of FcμR expression during B and T cell activation. Although this receptor was initially designated as Fas apoptotic inhibitory molecule 3, or TOSO, our results indicate that FcμR per se has no inhibitory activity in Fas-mediated apoptosis and that such inhibition is only achieved when anti-Fas antibody of an IgM but not IgG isotype is used for inducing apoptosis.

CORRESPONDENCE
Hiromi Kubagawa:
hiromikubagawa@uab.edu

Abbreviations used: 7-AAD, 7-aminoactinomycin D; APC, allophycocyanin; CLL, chronic lymphocytic leukemia; FAIM3, Fas apoptotic inhibitory molecule 3; FcR, Fc receptor; GPI, glycosylphosphatidylinositol; HRP, horseradish peroxidase; MFI, mean fluorescence intensity; MNC, mononuclear cell; pI, isoelectric point; pIgR, polymeric Ig receptor; PKC, protein kinase C; PLC, phospholipase C; SA, streptavidin.

IgM is the first Ig isotype to appear during phylogeny, ontogeny, and the immune response, and has been suggested as a first line of host defense to pathogens. Serum levels of IgM in mice raised under germ-free conditions are similar to those of mice maintained under conventional housing conditions (Haury et al., 1997). Thus, production of preimmune "natural" IgM antibody, primarily by $CD5^+$ B-1 cells, is likely to be regulated by mechanisms unrelated to exogenous antigen specificity. In contrast, antigen-induced IgM production is mainly derived from conventional B-2 cells. The importance of both natural and induced IgM antibodies in immune responses has been established through recent studies of a mutant mouse strain in which B cells expressing surface IgM and IgD could switch and secrete IgG and IgA, but not IgM, antibodies (Boes et al., 1998a; Ehrenstein et al., 1998). These mutant mice had impaired control of viral and bacterial infections because of inefficient induction of protective IgG antibody responses (Boes et al., 1998b; Ochsenbein et al., 1999; Baumgarth et al., 2000). Thus, these findings indicate that IgM antibody can profoundly influence immune responses and suggest that some of these effects are mediated by binding to effector molecules such as Fc receptor (FcR) and complement via its carboxyl-constant regions.

Several FcRs, namely FcR for IgG (FcγRI/CD64, FcγRII/CD32, and FcγRIII/CD16), IgE (FcεRI), and IgA (FcαR/CD89), have been characterized at both the protein and nucleic acid levels (Ravetch and Nimmerjahn, 2008).

H. Kubagawa, S. Oka, and Y. Kubagawa contributed equally to this paper.

The Rockefeller University Press $30.00
J. Exp. Med. Vol. 206 No. 12 2779-2793
www.jem.org/cgi/doi/10.1084/jem.20091107

In contrast, FcR for IgM (FcμR) has defied genetic identification, although the existence of FcμR on B, T, NK, and phagocytic cells has been suggested for >30 yr with variable and conflicting results (Basten et al., 1972; Moretta et al., 1975; Lamon et al., 1976; Ferrarini et al., 1977; Moretta et al., 1977; Pichler and Knapp, 1977; Santana, 1977; Haegert, 1979; Reinherz et al., 1980; Uher et al., 1981; Sanders et al., 1987; Mathur et al., 1988a; Mathur et al., 1988b; Ohno et al., 1990; Nakamura et al., 1993; Pricop et al., 1993; Rabinowich et al., 1996). In addition to the aforementioned classical FcRs, several other receptors expressed on unique cell types also bind Ig molecules: (a) neonatal FcR for IgG (FcRn) on intestinal epithelium, placenta, and endothelium (Roopenian and Akilesh, 2007); (b) low affinity FcεR (FcεRII/CD23) on B cells and macrophages (Conrad, 1990); (c) polymeric Ig receptor (pIgR) on mucosal epithelium (Kaetzel, 2005); and (d) FcR for IgA and IgM (Fcα/μR; Shibuya et al., 2000) on follicular dendritic cells (Kikuno et al., 2007). Although the latter two receptors bind polymeric IgA and IgM, their biochemical features and cellular distribution are distinct from those of the FcμR that we have previously characterized on B and T cells in humans (Sanders et al., 1987; Ohno et al., 1990; Nakamura et al., 1993). In this paper, we have identified a cDNA encoding a bona fide FcμR that is defined as transmembrane protein of ~60 kD expressed predominantly on B and T lymphocytes.

RESULTS

Molecular cloning of the FcμR

Our previous cellular and biochemical studies provided strong evidence for the existence of an FcμR that is expressed constitutively on chronic lymphocytic leukemia (CLL) B cells and inducibly on pre–B cell lines (Sanders et al., 1987; Ohno et al., 1990). To identify the gene encoding the putative FcμR, two different cDNA libraries from CLL B cells and a PMA-activated 697 pre–B cell line were constructed in a retroviral expression vector and then introduced into mouse T cell line BW5147. Transduced cells exhibiting IgM binding were enriched by FACS and subcloned. Many of the single cell–derived subclones from both cDNA libraries bound IgM (Fig. 1 A). RT-PCR analysis revealed that a DNA fragment of ~2 kb was specifically amplified only from IgM-binding subclones (Fig. 1 B), and their nucleotide sequence analyses defined an identical 1,173-bp open reading frame (CLL- and PMA-activated 697 pre–B cell–derived FcμR cDNA available from GenBank/EMBL/DDBJ under accession nos. GQ160900 and GQ160901, respectively; Fig. S1). Basic local alignment search technique database analysis revealed that the isolated FcμR cDNA was identical to that of the previously described human Fas apoptotic inhibitory molecule 3 (FAIM3; available from GenBank/EMBL/DDBJ under accession no. NM_005449), except for one nucleotide difference at a position reported as a synonymous single nucleotide polymorphism. FAIM3 was identified in a similar retroviral cDNA library–based functional assay as a potent inhibitor of Fas/CD95-induced apoptotic signaling and was originally designated as TOSO, after a Japanese liquor drunk on New Year's day to celebrate long life and eternal youth (Hitoshi et al., 1998). Interestingly, however, the apoptosis in this functional assay was induced by ligation of Fas with a mouse mAb of IgM isotype (CH11). This immediately raised the possibility that the CH11 mAb bound to the Fas via its Fabμ portion and to the FAIM3/TOSO via its Fcμ portion, thereby bringing them in close physical proximity in a process reminiscent of that described in FcγRIIb-mediated inhibition of BCR signaling by intact IgG anti-μ antibodies (Tony and Schimpl, 1980; Ravetch and Nimmerjahn, 2008).

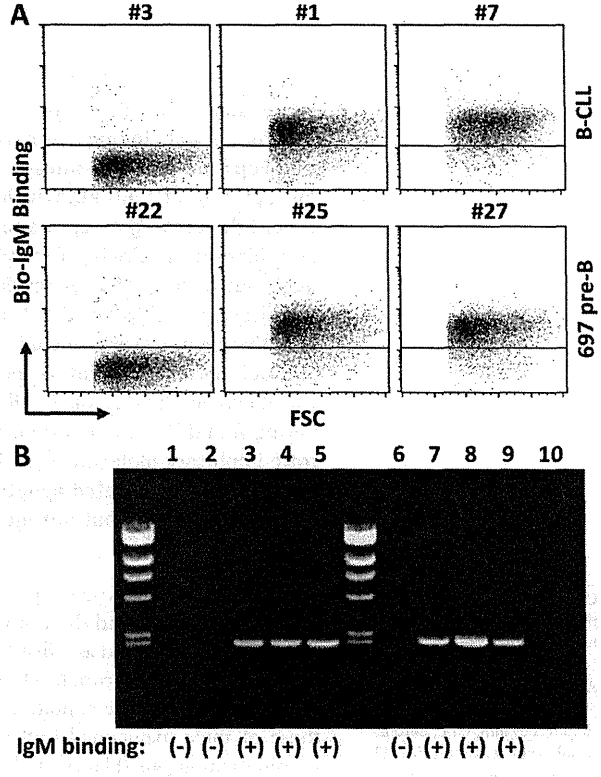

Figure 1. Isolation of IgM-binding subclones and identification of cDNA inserts. (A) Cells transduced by the retroviral expression construct containing CLL-derived (top) or PMA-activated 697 pre–B cell–derived (bottom) cDNA libraries were enriched for IgM binding by FACS and subcloned for limiting dilution. Three representative subclones from each library are shown for their IgM-binding activity or lack of binding, as determined by flow cytometry. (B) Agarose gel electrophoresis analysis of RT-PCR products. RNA isolated from nontransduced control BW5147 T cells (lane 1) and from IgM-binding (lanes 3–5 and 7–9) or IgM-nonbinding (lanes 2 and 6) subclones from CLL-derived (lanes 2–5) and PMA-activated 697 pre–B cell–derived (lanes 6–9) cDNA libraries were subjected to RT-PCR as described in Materials and methods. Amplified products were electrophoresed in 0.7% agarose and stained with ethidium bromide. Lane 10 is a PCR control without a first-strand cDNA template. *Hin*dIII-digested λ DNA was used as a size marker. The experiments were performed once for A and twice for B.

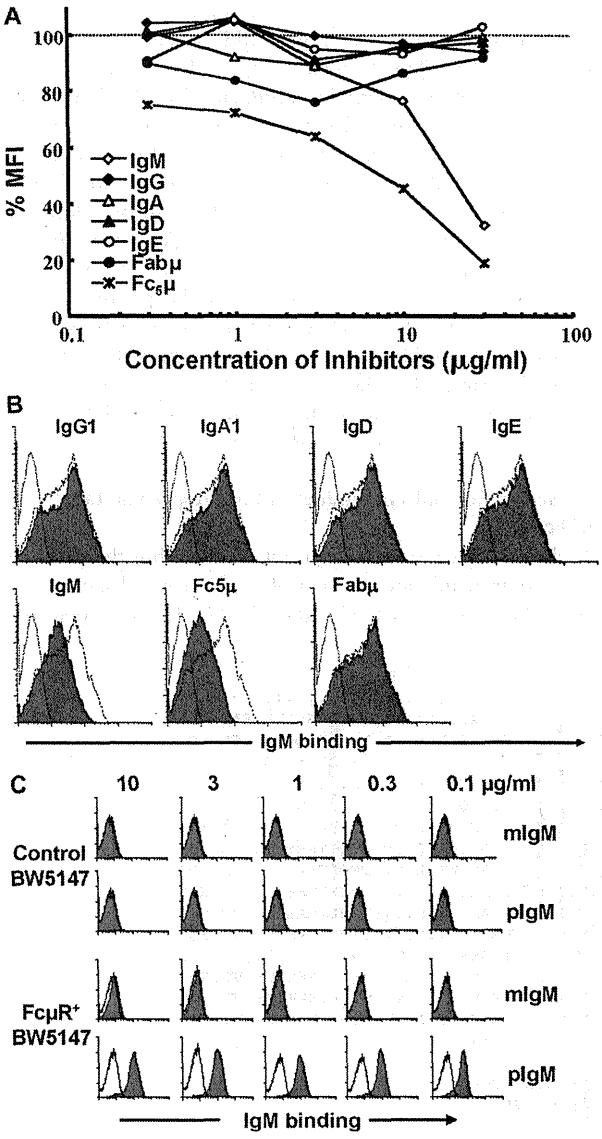

Figure 2. Evaluation of the Ig isotype specificity of the FcμR. (A) FcμR cDNA–transduced BW5147 T cells were preincubated with various concentrations of inhibitor paraproteins of human origin (IgM, IgG_{1-4}, IgA_{1-2}, IgD, IgE, Fabμ, and $Fc_5\mu$) and incubated with 4 μg/ml of biotin-labeled human IgMκ. Bound biotinylated IgM was detected by addition of PE-labeled SA. Stained cells were analyzed by flow cytometry. Results are expressed as the percent mean fluorescence intensity (MFI) estimated as follows: 100 × ([X of IgM binding with inhibitors − X of background control]/[X of IgM binding without inhibitors − X of background control]), where X indicates the MFI values. Because there were no significant differences among each subclass of IgG and IgA, the results from all four IgG subclasses and two IgA subclasses have been combined as IgG and IgA, and the mean values are presented for simplicity. (B) Representative binding inhibition profiles. FcμR+ BW5147 T cells were incubated first with an eightfold excess of the indicated inhibitor proteins and then with 4 μg/ml of biotin-labeled human IgMκ. The dotted, dashed, and continuous lines indicate the immunofluorescence profiles for background controls, IgM binding without inhibitors, and IgM binding with the test inhibitors, respectively. (C) Control and FcμR+ BW5147 cells were incubated with culture supernatants containing the indicated concentrations of monomeric (m) or pentameric (p) IgM anti-mouse RBC mAb before developing with biotin-labeled anti-mouse κ mAb and APC-SA. These experiments were performed at least twice.

The *FAIM3/TOSO* gene encodes a bona fide FcμR

To reconcile the conflicting functions of FAIM3/TOSO and our functionally defined FcμR, an ~1.2-kb cDNA containing the protein coding region of FAIM3/TOSO/FcμR was PCR amplified from PMA-activated 697 pre–B cells, subcloned along with a GFP cDNA into the bicistronic retroviral vector and then transduced into BW5147 T cells. The resultant GFP+ transductants clearly exhibited IgM binding (Fig. S2), thereby confirming that FAIM3/TOSO is an IgM receptor. The FcμR cDNA is predicted to encode a 390-aa type I membrane protein (17-aa signal peptide, 236-aa extracellular region, 19-aa transmembrane segment, and 118-aa cytoplasmic tail). The N-terminal half of the extracellular region contains a single V-set Ig-like domain with homology to both the pIgR and Fcα/μR (see next section), but the remaining extracellular region has no identifiable domain features (Fig. S3). There are no N-linked glycosylation motifs in the extracellular region, consistent with our previous biochemical characterization of the FcμR (Ohno et al., 1990). The mature core peptide is predicted to have an M_r of ~41 kD and an isoelectric point (pI) of ~9.9.

A quantitative inhibition immunofluorescence assay with various Ig isotypes and IgM fragments as inhibitors revealed that IgM and its $Fc_5\mu$ fragments consisting mostly of Cμ3/Cμ4 domains inhibited the binding of a biotin-labeled human IgM to FcμR+ BW5147 T cells in a dose-dependent manner, whereas the Fabμ fragments and other human Ig isotypes (IgG_{1-4}, $IgA_{1,2}$, IgD, and IgE) did not, thereby confirming the Fcμ specificity of the FcμR (Fig. 2 A). Fig. 2 B shows a representative inhibition profile for IgM binding with an eightfold excess of inhibitors. The inability of FcμR to bind polymeric IgA clearly indicates that FcμR is distinct from pIgR and Fcα/μR, both of which are shown to bind IgM and polymeric IgA. Moreover, the lack of binding to aggregated IgG further confirms the unique IgM isotype specificity of this receptor. Interestingly, mouse IgM bound better to the human FcμR than human IgM, and essentially identical FcμR binding was observed with IgMκ and IgMλ ligands irrespective of the presence of Ca^{2+}/Mg^{2+}. The affinity of IgM/FcμR binding was estimated by Scatchard plot analysis using ^{125}I-labeled human IgM and FcμR+ BW5147 T cells. Assuming a 1:1 stoichiometry of pentameric IgM ligand to FcμR, this analysis revealed a strikingly high binding affinity of 10.8 ± 9.2 nM (mean ± SD from four experiments with two different human IgM myeloma proteins). Pretreatment of FcμR+ cells with neuraminidase slightly enhanced IgM binding, suggesting a role of sialic acid in this interaction, as reported previously by others